LBL-31982
UC-132

Lawrence Berkeley Laboratory
UNIVERSITY OF CALIFORNIA

EARTH SCIENCES DIVISION

Seismic Imaging of the SWCC

T.M. Daley and E.L. Majer

January 1992

For Reference
Not to be taken from this room

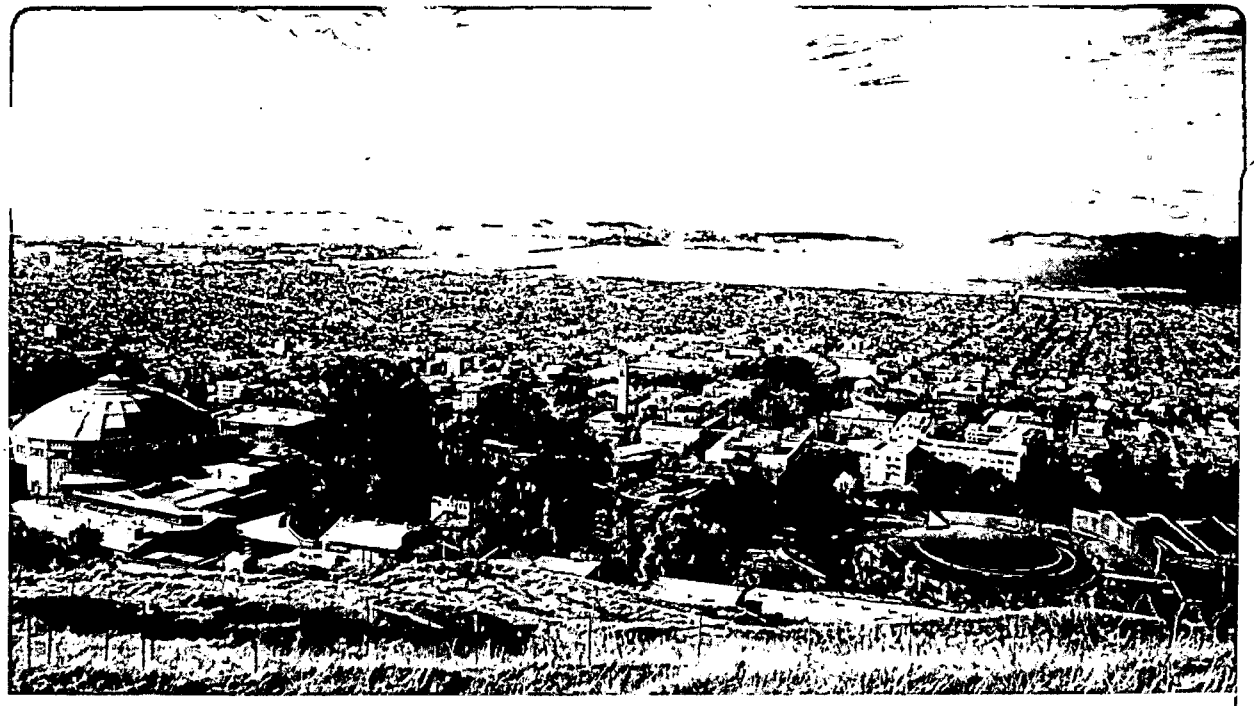

LBL-31982
Copy 1
Bldg. 50 Library.

Prepared for the U.S. Department of Energy under Contract Number DE-AC03-76SF00098

DISCLAIMER

This document was prepared as an account of work sponsored by the United States Government. Neither the United States Government nor any agency thereof, nor The Regents of the University of California, nor any of their employees, makes any warranty, express or implied, or assumes any legal liability or responsibility for the accuracy, completeness, or usefulness of any information, apparatus, product, or process disclosed, or represents that its use would not infringe privately owned rights. Reference herein to any specific commercial product, process, or service by its trade name, trademark, manufacturer, or otherwise, does not necessarily constitute or imply its endorsement, recommendation, or favoring by the United States Government or any agency thereof, or The Regents of the University of California. The views and opinions of authors expressed herein do not necessarily state or reflect those of the United States Government or any agency thereof or The Regents of the University of California and shall not be used for advertising or product endorsement purposes.

This report has been reproduced directly
from the best available copy.

Available to DOE and DOE Contractors
from the Office of Scientific and Technical Information
P.O. Box 62, Oak Ridge, TN 37831
Prices available from (615) 576-8401, FTS 626-8401

Available to the public from the
National Technical Information Service
U.S. Department of Commerce
5285 Port Royal Road, Springfield, VA 22161

Lawrence Berkeley Laboratory is an equal opportunity employer.

DISCLAIMER

This document was prepared as an account of work sponsored by the United States Government. While this document is believed to contain correct information, neither the United States Government nor any agency thereof, nor the Regents of the University of California, nor any of their employees, makes any warranty, express or implied, or assumes any legal responsibility for the accuracy, completeness, or usefulness of any information, apparatus, product, or process disclosed, or represents that its use would not infringe privately owned rights. Reference herein to any specific commercial product, process, or service by its trade name, trademark, manufacturer, or otherwise, does not necessarily constitute or imply its endorsement, recommendation, or favoring by the United States Government or any agency thereof, or the Regents of the University of California. The views and opinions of authors expressed herein do not necessarily state or reflect those of the United States Government or any agency thereof or the Regents of the University of California.

LBL-31982

Seismic Imaging of the SWCC

Thomas M. Daley and Ernest L. Majer

Earth Sciences Division
Lawrence Berkeley Laboratory
University of California
Berkeley, California 94720

January 1992

This work was supported by the Assistant Secretary for Fossil Energy, Morgantown Energy Technology Center, of the U.S. Department of Energy under Contract No. DE-AC03-76SF00098.

Seismic Imaging of the SWCC

Thomas M. Daley and Ernest L. Majer

Center for Computational Seismology,
Lawrence Berkeley Laboratory, University of California,
Berkeley, Ca.

Introduction

The Cascades mountain range of southern Washington is a geologically complex and tectonically active region. The area has been explored for potential oil and gas reserves by several major oil companies, but exploration efforts (mostly electrical and seismic reflection surveys) are hampered by the geologic complexity which often leads to poor data quality. Although no commercial quantities of oil or gas have been found to date, the existence of major sedimentary basins and potential source rocks has lead to continued interest. The Department of Energy and the U.S. Geological Survey have conducted geophysical studies in the southern Washington region to study possible petroleum-bearing sedimentary basins as well as crustal tectonic structures. The natural gas potential of deep sedimentary basins is an area of research supported by the Morgantown Energy Technology Center of DOE's Office of Fossil Energy. This report summarizes the work to date which has been conducted at LBL's Center for Computational Seismology.

A major goal of our work is to investigate the seismic reflection characteristics of a possible marine sedimentary basin located between Mt. Rainier and Mt. St. Helens. The zone of interest was initially identified by magnetotelluric studies (Stanley et. al., 1987) as an anomalous conductor called the southern Washington Cascades conductor (SWCC). Stanley and others proposed that this conductor "might represent an accretionary prism/forearc basin system that was compressed during accretion of an extensive seamount assemblage"(Stanley, et. al., 1991). This interpretation is largely based on correlation of shallow parts of the conductor with outcrops of Eocene marine and transitional rocks, as well as the regional tectonic setting of the SWCC. The possibility of the SWCC containing hydrocarbon reservoirs was discussed in detail by Stanley, et. al. (1991). As part of our research we have studied several aspects of seismic imaging of the SWCC. Our work has included ray tracing and synthetic seismograms generated for planning and interpretation of explosive shots using a 1024 channel sign-bit acquisition system; a comparison of the signal strength and imaging capabilities of explosive and vibroseis sources, and processing and interpretation of one of a series of seismic reflection surveys conducted over the SWCC with the sign-bit recording system.

Background

Basic research into the possible exploitation of deep gas includes identifying areas in which natural gas could be generated and trapped in sediments which have been carried to depth by subduction processes. The western Cordillera of North America, with multiple subduction zones, has been the site of reconnaissance surveys designed to locate sedimentary formations which have been placed deep in the crust (15000 feet or more). The accretionary prisms and forearc basins which form in conjunction with subduction zones have the potential for large accumulations of marine and continental organic material. This material could then be a deep hydrocarbon source for reservoir rocks. While basic studies of this topic include hydrocarbon generation, geochemistry and the detailed stratigraphy of subduction, the geophysical studies focus on characterization of sedimentary basins which could be source rock or reservoir rock and the delineation of geologic structures which are possible traps for hydrocarbons.

One area identified as a site for the subduction of marine sediments is the southern Washington Cascades where the Juan de Fuca plate is subducting beneath the North American plate. Trapped between the two plates are sedimentary rocks, volcanic rocks and oceanic crustal slices. An initial attempt to identify potential sedimentary basins used magnetotelluric (MT) surveys which determine the electrical conductivity of subsurface material by measuring naturally occurring electric and magnetic fields at the surface of the earth. MT measures conductivity (or its inverse, resistivity) as a function of frequency. By converting frequency-resistivity functions to earth response functions, one obtains conductivity as a function of depth. Typically, one dimensional inversions are performed at each MT site and the results are combined into a cross-section. 2-D inversions are often performed on stations along a line using the 1-D results as an initial model. MT surveys conducted in the southern Washington area outlined an anomalous conductivity zone with resistivities of less than 5 ohm-m at depths as shallow as 3 km (Stanley, et. al. 1987). These values compare to nearby formations with resistivities of 150 to 500 ohm-m which are interpreted as andesitic volcanic rocks, mafic oceanic crust and basalts. The low resistivity (high conductivity) anomaly named the Southern Washington Cascade Conductor is postulated as a possible sedimentary basin accreted during subduction (Stanley, et. al. 1991). This hypothesis is supported by observation of Eocene marine rocks of the McIntosh Formation which outcrop where the SWCC becomes shallow to the west. Alternate causes and lithologies of the conductive zone such as geothermal fluids, authigenic minerals or pre-Tertiary, carbonaceous metasedimentary rocks, are discussed by Stanley, et. al. (1991).

The regional setting of the SWCC is complex because of the active tectonic forces. Both intrusive bodies and structural deformation are complicating factors in defining the SWCC. A simplified geologic map of the area is shown in Fig. 1. An active seismic zone on the west side called the St. Helens Zone (SHZ), (Weaver and Smith, 1983) is inferred to have a narrow magma body rising beneath Mt. St. Helens (Fig. 1). The SWCC is overlain by thick volcanic

flows of the Ohanapecosh and Stevens Ridge formations which are Miocene and Oligocene age (25 - 40 Ma). These volcanics form one of the hinderances to good seismic reflection data (other seismic problems include highway noise and complicated recording geometry). The basement underlying the SWCC is unknown but is proposed as subducting oceanic crust along the western margin. There are two major anticlinal structures identified above the SWCC. The Morton anticline (MA in Fig. 1) is near the western edge of the SWCC and the Skate Mountain anticline is near the eastern margin. These anticlines could serve as structural traps for hydrocarbons.

Stimulated by the MT modeling, commercial well data, nearby seismic surveys (reflection and refraction), regional gravity and magnetic surveys, geologic sections constructed by the state of Washington, and estimates of organic content and maturation in nearby sediments (Westhusing and Krehbiel, 1990), the Dept. of Energy began a series of seismic reflection profiles. The seismic profiling began in 1988, and 6 lines using a 1024 channel, sign-bit recording system and vibroseis sources have been completed (Fig. 2).

Ray Tracing

Initial attempts at modeling the seismic response of SWCC with ray tracing were conducted in conjunction with the planning of dynamite shots on reflection lines 1 and 2 (Fig. 2). It was hoped that a dynamite source would provide enough energy to determine the reflection characteristics of the SWCC in a single shot gather and provide greater resolution at depth than the vibroseis data. The goal of the ray tracing was to help interpretation of the proposed dynamite shots and to aid in the selection of shot locations. Ray tracing can give expected travel times for reflections and an indication of the subsurface coverage of seismic rays for each interface in the model. In particular, we hoped to find the travel times and ray coverage for the top of the SWCC and for the top of the proposed subducting oceanic crust. In addition to travel times, synthetic seismograms were computed for comparison with the dynamite data to be acquired.

The 2-D dynamic ray tracing package BEAM87 (Cerveney, 1977) was used to model sources at a series of surface shot points with 20 receivers at 1 km spacing. The geologic model used for ray tracing was derived from the MT interpretation and initial interpretation of seismic reflection line 1. Two variations of the model were studied, one with the SWCC top having an anticline corresponding to the surface expression of the Morton anticline (Fig. 3a) and one without an anticlinal top to the SWCC (Fig. 4a). We hoped to see if an anticline feature on SWCC could be detected in a single shot gather. The seismic velocities used in this modeling were derived from initial reflection processing and previous refraction surveys. The shallow volcanics of the Ohanapecosh and Stevens Ridge formation were assigned velocities of 5.5 km/s, the Puget Group (nonmarine sedimentary rocks) were given a linear gradient from 4.5 to 5.2 km/s, the SWCC was given a linear gradient from 5.0 to 6.0 km/s and 6.5 km/s was used for proposed subducting oceanic basalts of the Crescent Formation (Stanley,

personal communication).

Fig. 3a, 3b and 3c show, respectively, the raypaths for reflections from the tops of the Puget group, the SWCC, and the Crescent formation. Fig. 4a, 4b and 4c are the same but without an anticline for the SWCC. The shot point is near the middle of reflection line 5, above the Stevens Ridge volcanics. Fig. 3b and 3c show that this shot location would give good coverage of the SWCC and Crescent formation west of the Morton Anticline. Comparing 3b and 4b, we see that an anticlinal SWCC will give a slight triplication of travel times. This affect would probably be seen in field data as increased energy in the SWCC reflection at the receivers west of the Morton anticline, caused by the arrival of overlapping wavelets. Fig. 3d and 4d show the synthetic shot gathers computed for the two models (only the receivers east of the shot are shown). The SWCC reflection begins later in 3d (without anticline) but advances to earlier time to the east. The Crescent formation reflection is seen at times as early as 2.2 s. From the various source locations which were modeled, we determined that the 3 best shot locations for imaging the SWCC would be centered on the Morton anticline and about 10 km west and east.

Comparison of Explosive and Vibroseis Sources

During the acquisition of reflection line 5, 4 explosive shots were recorded while the 20 km line was in place. The shot point for all 4 shots was about 1/2 mile off the east end of the east-west portion of line 5 (Fig. 2). In addition, a vibroseis shot gather was recorded at the same location with 4 sets of 5 source sweeps recorded (20 sweeps total). Line 5 was recorded with 12 sweeps at each shot point. By comparing the 4 shot explosive stack (Fig. 5a) with a 48 sweep vibroseis stack (Fig. 5b) and a 12 sweep vibroseis stack (Fig. 5c), we can judge the relative signal-to-noise ratio attained by each one. Looking just at the first arrival (0.2 to 2.8 s), it is clear that the explosive shot (Fig. 5a) has the most energy and the best signal-to-noise ratio. It should be noted that since the explosive data was acquired with a sign-bit data acquisition system, the amplitude sensitivity (the number of digital amplitude steps in the data) is equal to the number of shots stacked plus one. For one shot of sign-bit data, both signal and noise would have an amplitude of -1 or +1. A stack of 4 sign-bit explosive recordings would have range of amplitudes from -4 to 4. This means that the noise preceding the first arrival will appear to have higher amplitudes when there are fewer stacks. With vibroseis data, which is the usual sign-bit application, the use of a correlation operator (the source sweep) creates an amplitude range related to the length of the operator. This gives a typical amplitude range of +/- 36,000 for vibroseis data while allowing the large number of data channels possible with sign-bit recording.

Comparing the two vibroseis data sets, the stack of 48 (Fig. 5b) does have significantly better signal-to-noise ratio than the stack of 12 sweeps (Fig. 5c). This is especially clear on the western part of the spread where the 12 sweep stack does not even show the direct arrival. Unfortunately, neither the 48 sweep vibroseis stack or the 4 shot explosive stack show

identifiable reflections. Only direct arrivals and reverberations can be seen. Attempts to enhance possible reflections by dip filtering direct arrivals proved unsuccessful: Only the east-west part of the line was dip filtered because the north-south portion had too much variation in source-receiver offset for the transformation to frequency-wavenumber domain (Fig. 6). Apparently, even more energy (more shots) is necessary to use a single shot gather for subsurface imaging in this area. In fact, the shot point used for this study appears to give better energy transmission than much of line 5. A typical line 5 shot gather with 12 vibroseis sweeps is shown in Fig. 7; as can be seen the direct arrival is only transmitted 7 km away from the shot point. This is much poorer energy transmission than the 12 sweep record from the explosive shot location.

Reflection Line 5

A total of 40 km of seismic reflection data was obtained with Line 5. Our processing and interpretation used a 20 km section which overlaps lines 1 and 2 for about 12 km west of the Morton anticline and then turns north for about 8 km into the strike direction of the SWCC (Fig. 2). The geophone spacing was 20 m, about half the spacing of most of lines 1 and 2, and the source spacing was 40 m. Fig. 8a shows the shot point geometry. This geometry gives a cdp trace about every 10 m. The vibroseis sweep was a 39 to 9 Hz 15 s sweep, with 5 vibrator trucks and 10 s of correlated output. Processing work was performed by Geotrace Technologies (formerly Daniel Geophysical), and at LBL, under subcontract from the acquisition contractor Geosystems.

Initially we used all 1024 channels (20 km) in a cdp gather, but this approach was quickly discarded. Not only did the severe bend to the North make all 2D assumptions incorrect, but the typical data quality from an individual shot gather did not justify using receivers more than 4 km away from the source (see Fig. 7). Therefore, we limited our present study to the east-west portion of line 5, shotpoints 962 to 1520. This section of line 5 approximately coincides with line 1 and the west end of line 2.

In the next processing attempt for this section of line 5, we used 270 traces per shot (5.4 km), and broke the east-west section into 3 parts. The reduced number of traces per shot was dictated by the lack of energy in a single shot, the crookedness of the line and the large amounts of computer memory necessary for 10 seconds of multi-channel data. The midpoint line was heavely smoothed to produce a reasonable number of traces per cdp. For the midpoint line shown in Fig. 8b, which is the western 5 km of line 5, the average cdp fold is about 140 for the 270 trace shots. An initial brute stack was produced using surface statics and a velocity model from lines 1 and 2 (Fig. 9). This stack is very poor quality with no coherent events after 1 second. Further velocity analysis of the cdp gathers again demonstrated the lack of coherent energy. Fig. 10 shows a velocity semblance plot generated for consecutive cdps over a velocity range of 2 to 10 km/s. The velocity semblance is generated by stacking the cdp traces at a series of stacking velocities and computing the amplitude and cross-correlation coefficient (semblance) in a time window for each velocity and then

contouring the amplitudes as a function of velocity and time along the trace. As can be seen in Fig. 10, there is little coherent energy below 4 or 5 seconds. This observation holds true for all the velocity analysis performed along line 5.

Initial analysis of the brute stack showed that there was significant areal smearing of midpoints along the line. This is caused by the crookedness of the line and it leads to reflection points spread over a large area being stacked together into a single cdp trace. In order to gauge the error introduced by this midpoint smearing, we constructed a 48 channel (960 m) shot gather for the western 4.5 km of line 5 (112 shots). The midpoint distribution for this geometry is shown in Fig. 11. The midpoints for the 48 channel stack fall along the cdp line, giving a truer 2D reflection profile. A brute stack of the 48 channel cdp line is shown in Fig. 12. While the data quality is still very poor, there is less stretching of traces, and reflection segments in the first second appear more coherent. There are more reflection segments on the 270 channel gather, and while this may be partially due to the increased signal-to-noise ratio from the larger fold values, it also represents the effect of reflection midpoints being spread over a 3D volume instead of along a 2D line. The complicated geology of the area is clearly three-dimensional, and any smearing of midpoints away from the cdp line will lead to out of plane reflections being imaged into the line. Fig. 13 shows a detailed comparison of the 270 channel and 48 channel stack, and the improved resolution of the 48 channel stack is evident for those events which are common to both stacks.

Because of the poor overall data quality, both for individual shot gathers (Fig. 7) and for brute stacks (Fig. 9), it is clear that simple cdp processing will not produce a useful section for interpretation. More complicated processing was performed by Geotrace Technology. They used intensive prestack processing including time varying spectral whitening, time varying AGC (automatic gain control), multiple passes of residual statics (surface consistent and nonsurface consistent) and velocity analysis, multichannel deconvolution for enhancing dipping events and DMO (dip moveout) analysis (Brad Feild, Geotrace, Pers. Com., 1991). Their cdp stack was limited to midpoints which fell near the cdp line (giving the 2D imaging we attempted but with potentially more traces per cdp), and the shot gathers were limited to +/- 2 km offset because of the lack of energy in each shot and the crooked line geometry. Unfortunately, because many of their processing algorithms are proprietary and because we have not yet received a detailed processing description, it is difficult to judge the extent to which their processing may distort or force events into the final stacked section. Nonetheless, the section recently provided by Geotrace (Fig. 14), gives an apparently much improved image of the east-west portion of line 5. This section is quite similar to the coincident section of lines 1 and 2 which were processed by Golden Geophysical with different processing techniques (Stanley, et. al. 1991).

Using the Geotrace processing, it is possible to interpret line 5 in terms of the model proposed from the MT studies of the SWCC and earlier interpretations of lines 1 and 2 by Westhusing and Krehbiel (1990) who looked at a subduction model and a rifted basin model.

Line 5 appears to support the subduction model since a fairly continuous zone of eastward dipping events (interpreted as the top of the Crescent formation) crosses the section from 2.5 s on the west end to 4.0 s on the east (Fig 14). The interpretation shown in Fig 15a is based on analysis by Stanley, et. al. (1991), who had a continuous section of conductive rocks (the SWCC) on top of the Crescent formation and projected them to thin out and coincide with surface outcrops of the McIntosh formation in the Bear Canyon area west of line 5. Following this model, we interpret a faulted synclinal boundary between the Puget Group and the SWCC from 0.9 to 1.5 s, and an SWCC/Crescent Formation boundary dipping west to east from 2.0 to 3.5 s (Fig. 15a). This interpretation is quite plausible, however it does leave several strong reflection events within the SWCC including one which intersects the top of the Crescent Formation between 2.0 and 2.5 s. This indicates the SWCC contains discrete blocks of conductive material and we are imaging the boundary between two such blocks as it intersects the top of the Crescent Formation.

Fig. 15b shows an alternate interpretation of line 5 which assumes the SWCC pinches out at depth instead of surfacing to the east. A shallow zone of reflectivity between 0.5 and 1.2 s is interpreted as the boundary between the Stevens Ridge volcanics and the underlying Puget group. The SWCC is interpreted as a wedged section on the east side between the Puget group and the Crescent formation with an apparent pinchout in the center of the section. This model of a pinchout of the SWCC is primarily based on the coincidence of line 5 with decreasing magnitude of the MT anomaly (Fig 2), however the current work of Stanley et. al. (1991) does extend the SWCC to the surface west of line 5 with a vertical boundary east of Bear Canyon. If the SWCC does pinchout under line 5, the 2.0 s two-way time to the top would represent a depth of 2.5 to 3 km.

Summary

Starting with a geologic model based on MT and other information, our raytracing demonstrated that the SWCC could be imaged with the acquisition geometry used for the seismic profiling. However, differences between geologic models could be difficult to see with single shot gathers. For example, removing the anticline structure from the SWCC leads to the differences in synthetic seismograms seen in Fig. 3d and 4d. These differences would require data with much greater signal-to-noise ratio than any so far acquired. The next attempt at modeling should include 3D structures, since it is likely that 3D effects are of first order importance. It is possible that future processing of the north-south portion of line 5 will lead to an estimation of 3D seismic response of the SWCC.

Comparison of the explosive and vibroseis sources demonstrated that the explosive source gives greater energy. With the explosive source, the direct arrival is extended across the 20 km spread. The 12 sweep vibroseis stack is much too weak for the 20 km spread, with perhaps 8 km of data being useful. The 48 sweep vibroseis stack was more comparable with the explosive source. While the shotpoint off the east end of line 5 gave greater energy

transmission than the nearest shot point on line 5, there was still insufficient energy reflected to allow analysis of single shot gathers.

The cdp analysis of line 5, like all other data collected in the Cascades, is hampered by near surface volcanics and consistently poor energy transmittal into the subsurface. The intensive prestack processing performed by Geotrace does give an interpretable section, which compares well with the coincident parts of lines 1 and 2. While it is difficult to estimate the reliability of reflections without more details of the Geotrace processing, the processed section does appear to support a subduction model. Two interpretations of line 5 are presented which show possible variations in the structure of the SWCC. The lithology and structure of the SWCC is still impossible to determine exactly without some well control, but if the top of the SWCC is the horizon shown in either Fig 15a or 15b, then it should be possible to propose a realistic drilling target.

Acknowledgements

This work was supported through U.S. Department of Energy Contract No. DE-AC03-76SF00098 by the Office of Fossil Energy, Morgantown Energy Technology Center. The authors would like to thank W.D. Stanley, W. J. Gwilliam, G.V. Latham and D. Hollis for their technical assistance.

References

Cerveny, V., I.A. Molotkov, and I. Psencik, *Ray Method in Seismology,* Charles University Press, Prague, 1977.

Stanley, W. D., W. J. Gwilliam, G. Latham and K. Westhusing, 1991, *Are Hydrocarbon Source Rocks Buried Beneath Volcanic Flows In The Southern Washington Cascades?,* U.S. Geologic Survey, Open File Report 91-119, 1991, In Press.

Stanley, W.D., C.A. Finn, and J.L. Plesha, 1987, *Tectonics and conductivity structures in the southern Washington Cascades,* Jour. Geophys. Res., 92, B10, v10, p10179-10193.

Westhusing K. and S. Krehbiel, 1990, *Exploration For Deep Source Hydrocarbons in Subduction Terrain Of the Pacific Northwest,* in Proceedings of the Natural Gas Research and Development Contractors Review Meeting Nov 1990, U.S. DOE Office of Fossil Energy, Morgantown W. Va., DOE/METC 91/6117, p162-184.

Weaver, C.S. and S.W. Smith, 1983, *Regional tectionic and earthquake hazard implications of a crustal fault zone in southwestern Washington,* Jour. Geophys. Res., 88, p10371-10383.

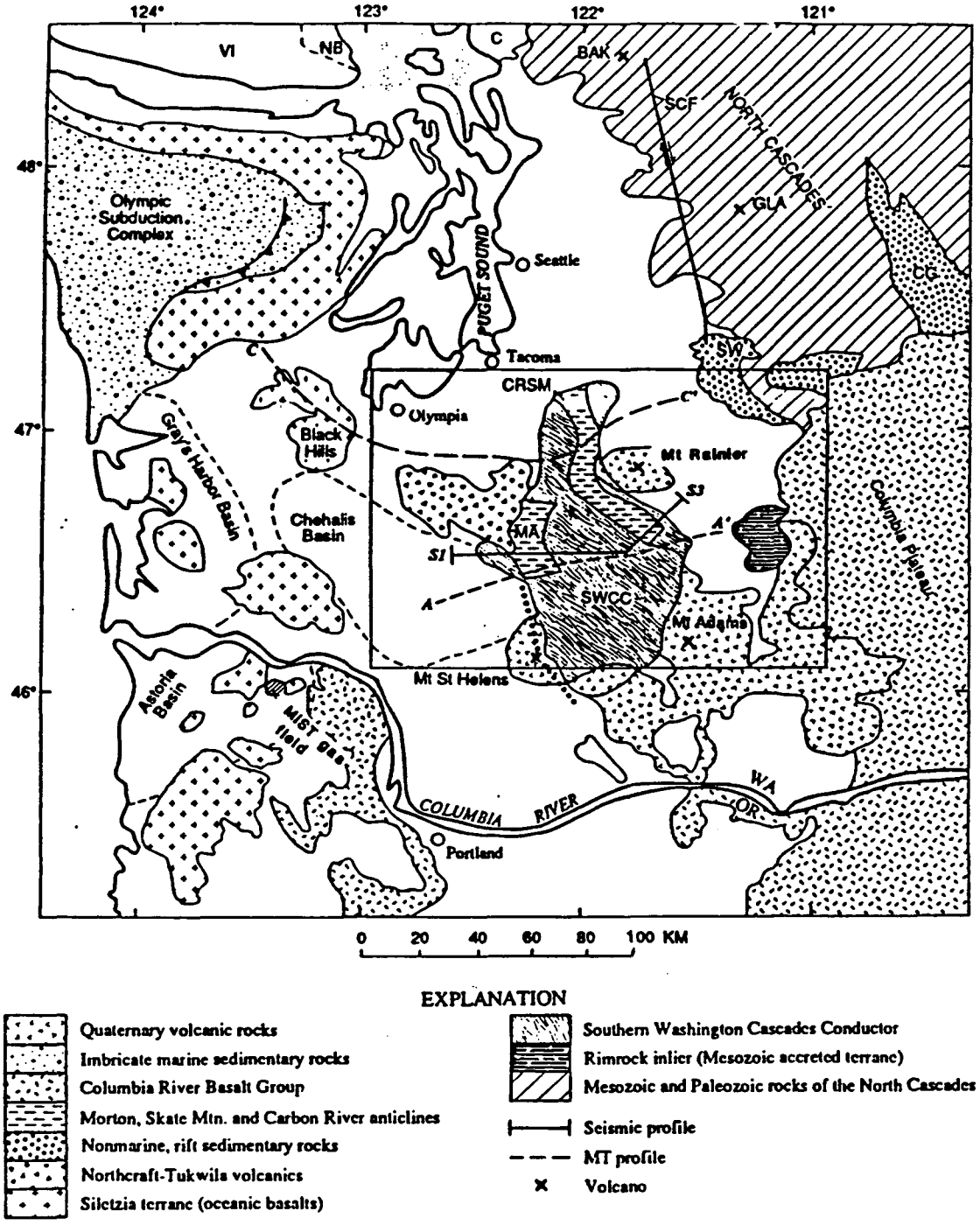

-Index geologic map for parts of Washington and Oregon. Among the key features noted are: the main late Tertiary basins of the region, outcrops of the basalt flows of Siletzia (accreted seamount complex), thick conductor mapped with MT surveys (SWCC), Mesozoic inlier (Rimrock inlier), anticlines in SWCC region (wide dotted lines, CRSM and MA), location of Mist gas field (in NW Oregon), MT (bold dashed lines, AA' and CC') and seismic (bold solid line, S1-S3) profiles. Area of detail shown in Fig. 2 is outlined by the box. SCF=Straight Creek fault, SWCC=southern Washington Cascades conductor, AST=Astoria Basin, GH=Grays Harbor Basin, VI=Vancouver Island, NB=Nanaimo basin, CG=Chiwaukum graben, SW=Swauk basin, C=Chuckanut basin, R=Rimrock Lake inlier, BAK=Mount Baker,GLA=Glacier Peak, PS=Puget Sound, MA=Morton anticlines, CRSM=Carbon River and Skate Mountain anticlines,SHZ=St. Helens seismic zone (bold line near Mt. St. Helens), SILZ=Siletzia, TUK=Northcraft and Tukwila Formations, CRB=Columbia River basalt Group, HV=Holocene volcanic rocks.

Fig. 1 Figure and caption from Stanley (1991).

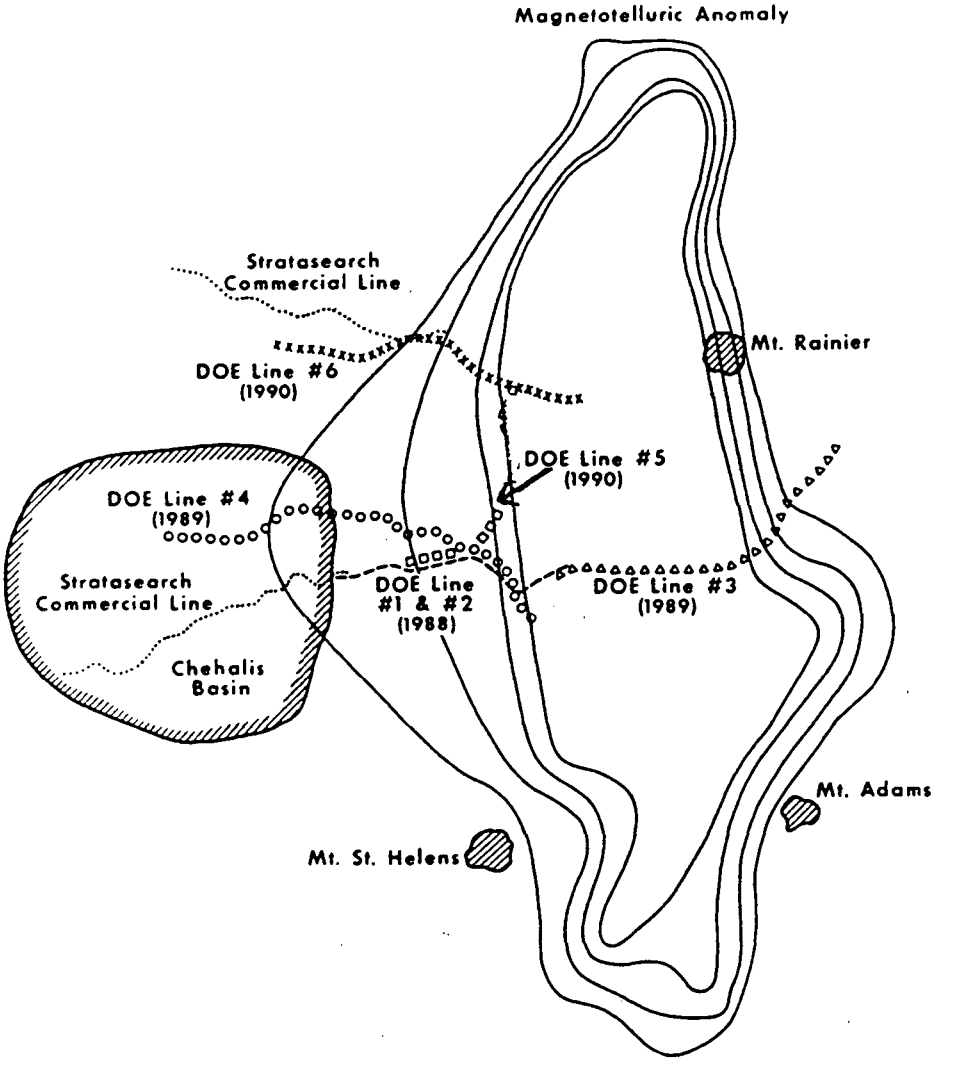

Fig. 2 Location map of seismic lines and MT anomaly, from Westhusing and Krehbiel (1990).

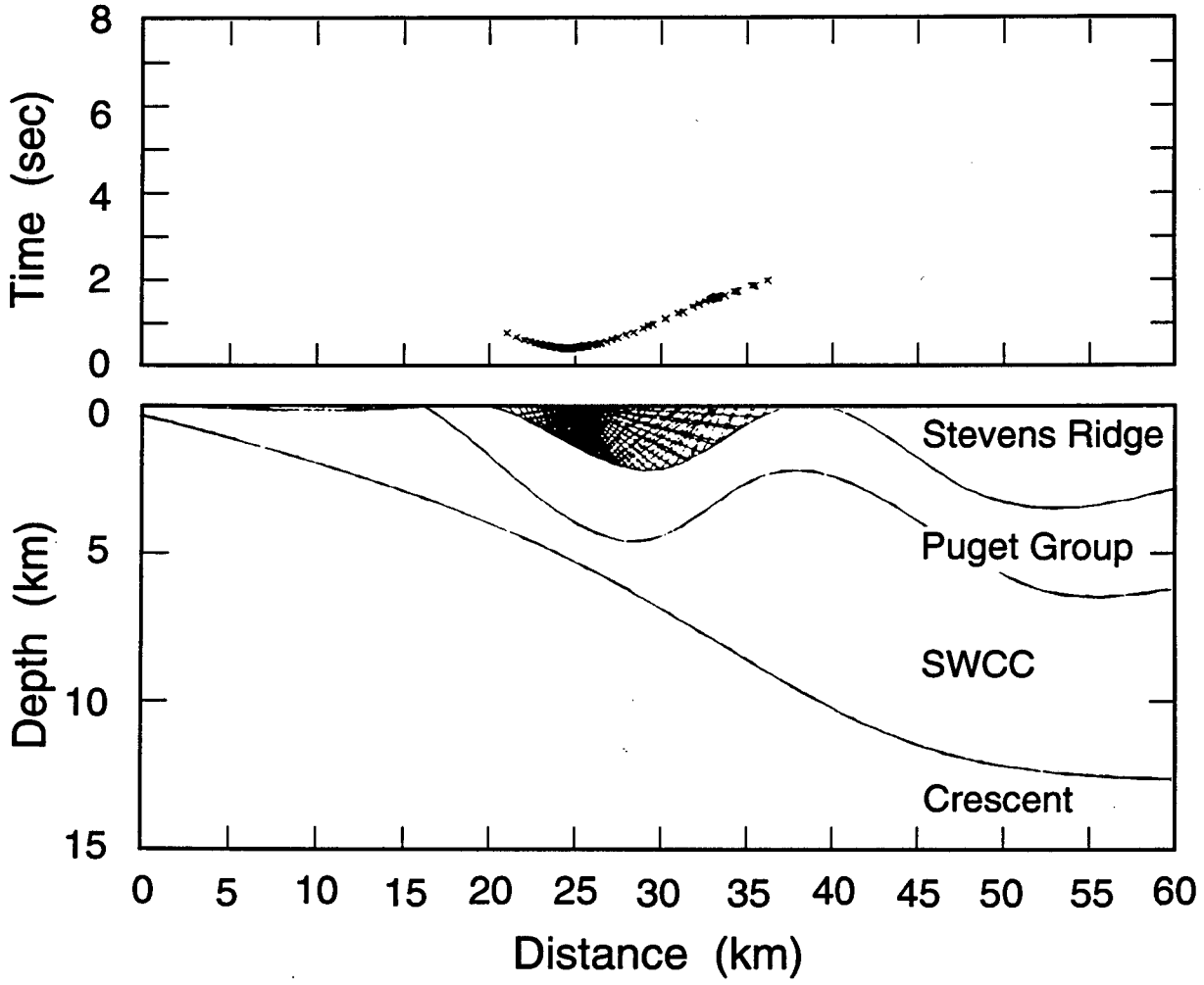

Fig. 3a Seismic rays and travel times for Stevens Ridge/Puget Group interface using subduction model with anticline for SWCC. Velocities are given in text.

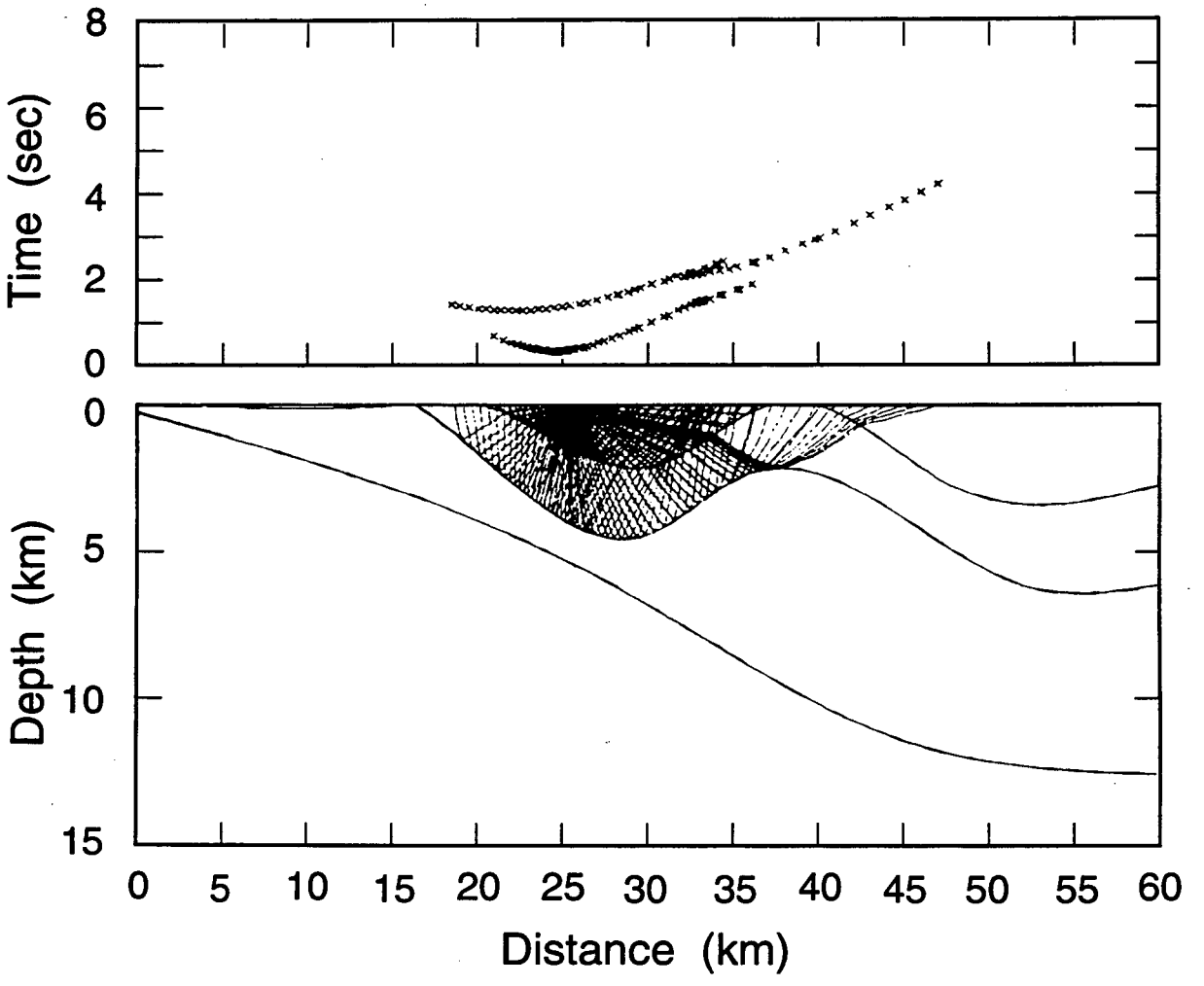

Fig. 3b Seismic rays and travel times including Puget Group/SWCC interface using subduction model with anticline for SWCC. Velocities are given in text.

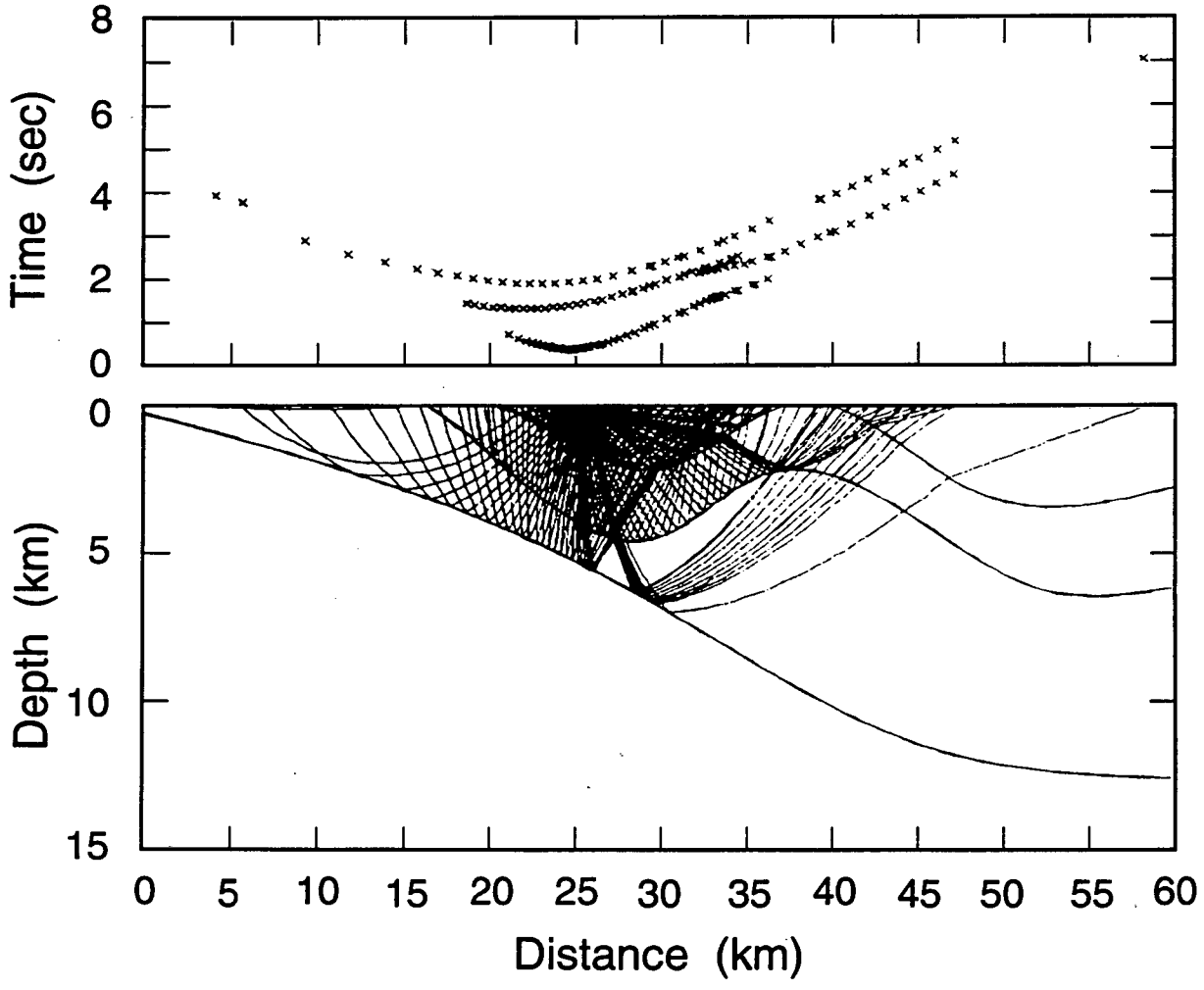

Fig. 3c Seismic rays and travel times including SWCC/Crescent interface using subduction model with anticline for SWCC. Velocities are given in text.

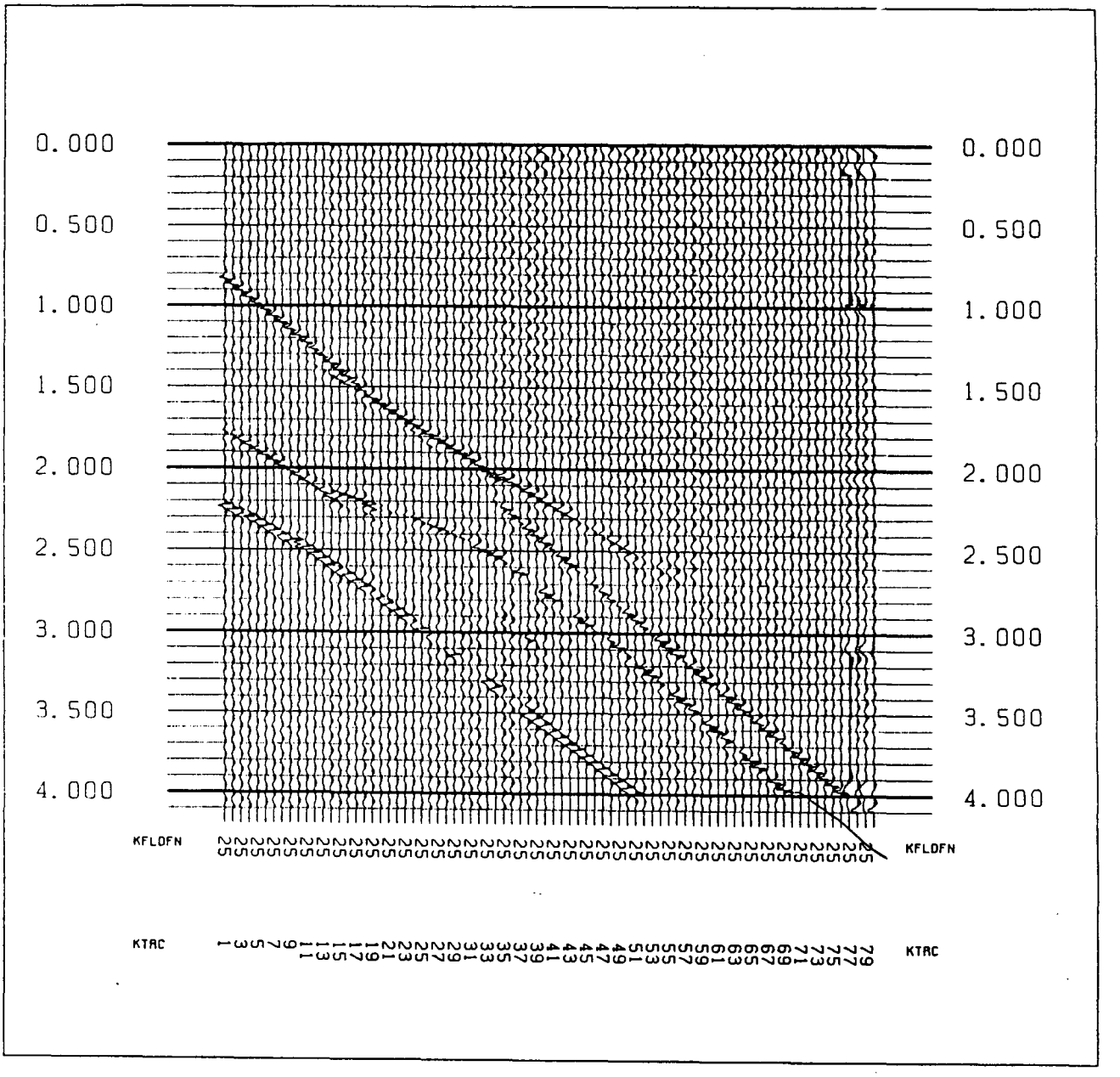

Fig. 3d Synthetic seismograms for source rays in Fig.3c, AGC applied. Traces are spaced every 250 m east of the source.

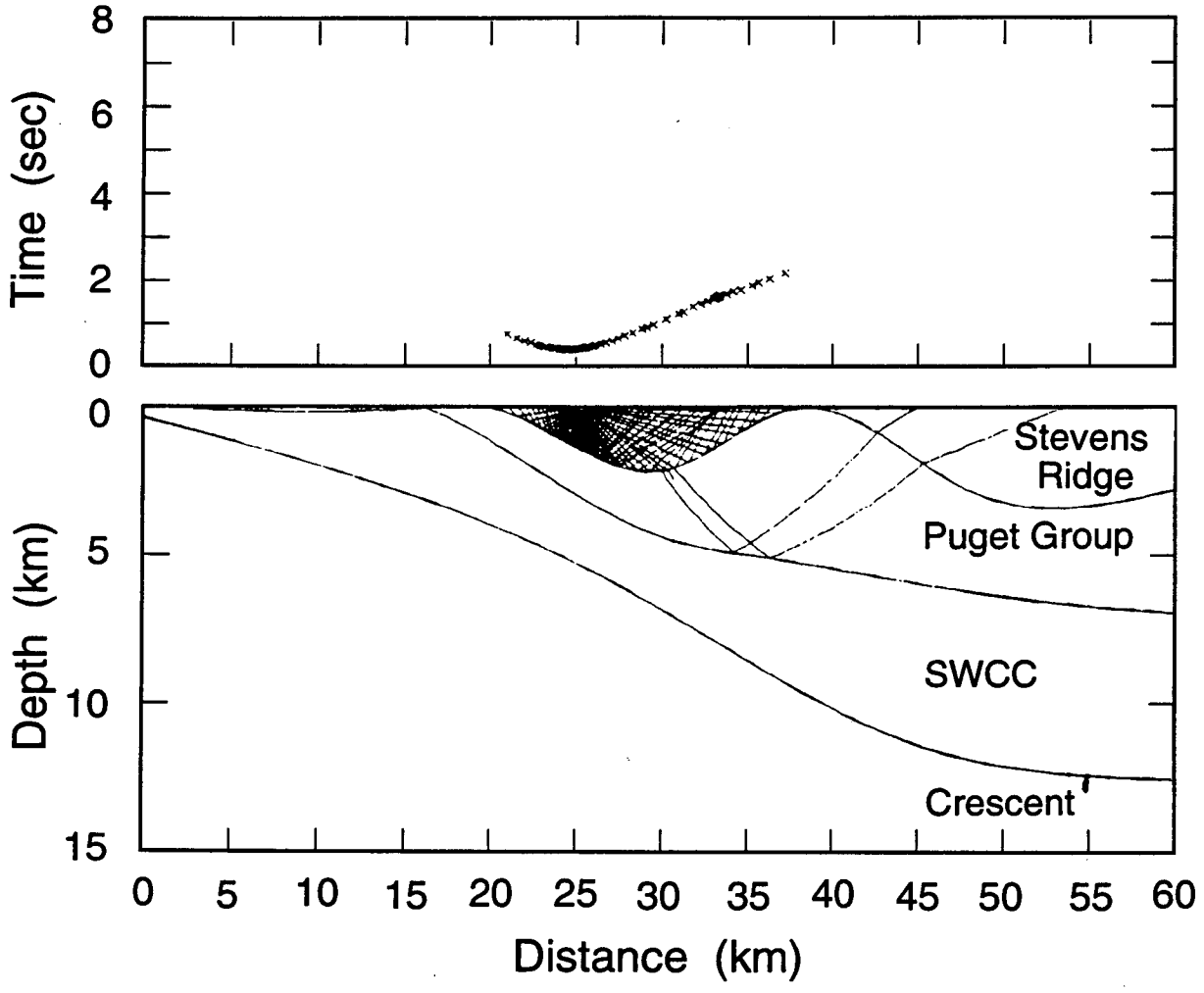

Fig. 4a Seismic rays and travel times for Stevens Ridge/Puget Group interface using subduction model without anticline for SWCC. Velocities are given in text.

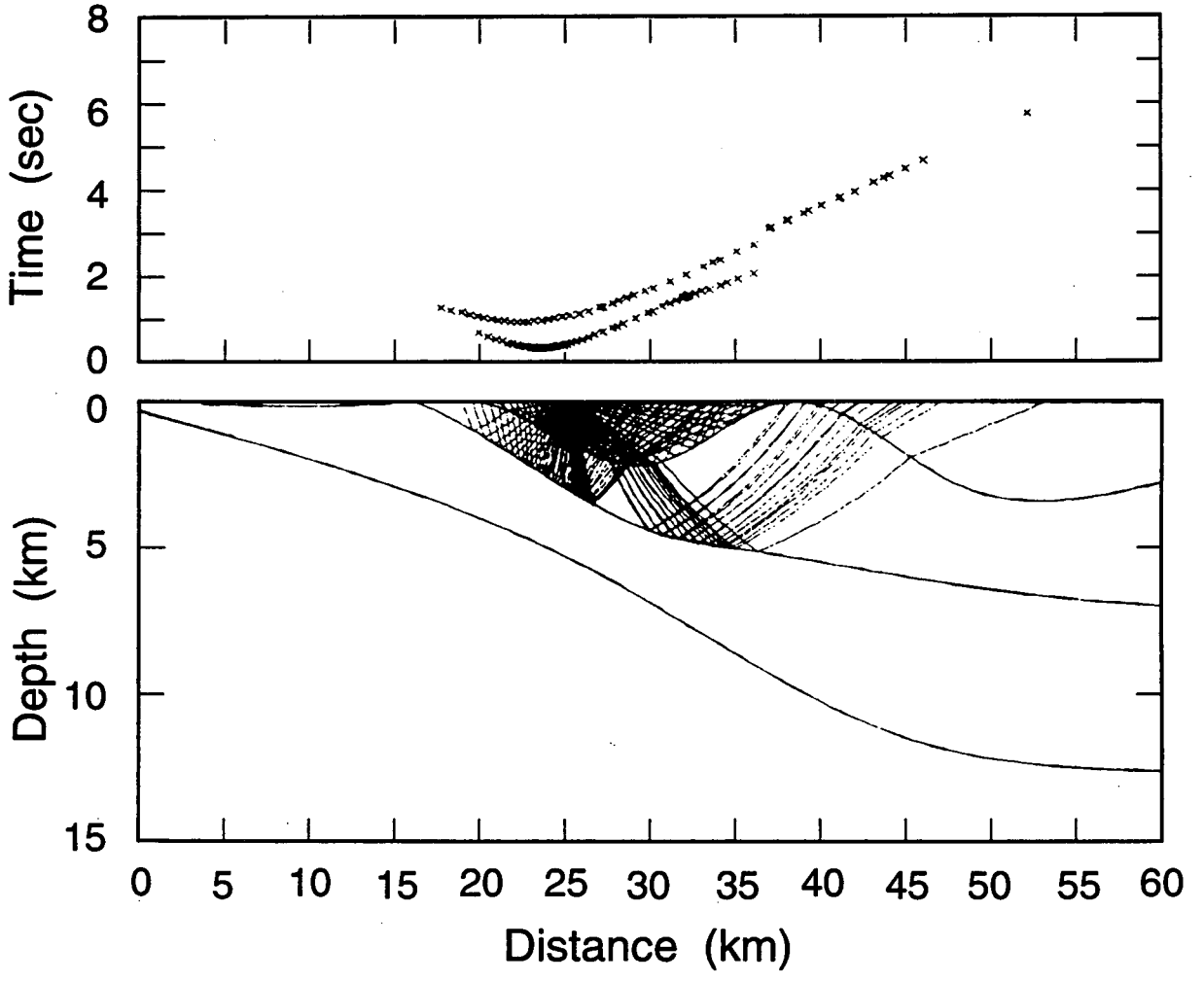

Fig. 4b Seismic rays and travel times including Puget Group/SWCC interface using subduction model without anticline for SWCC. Velocities are given in text.

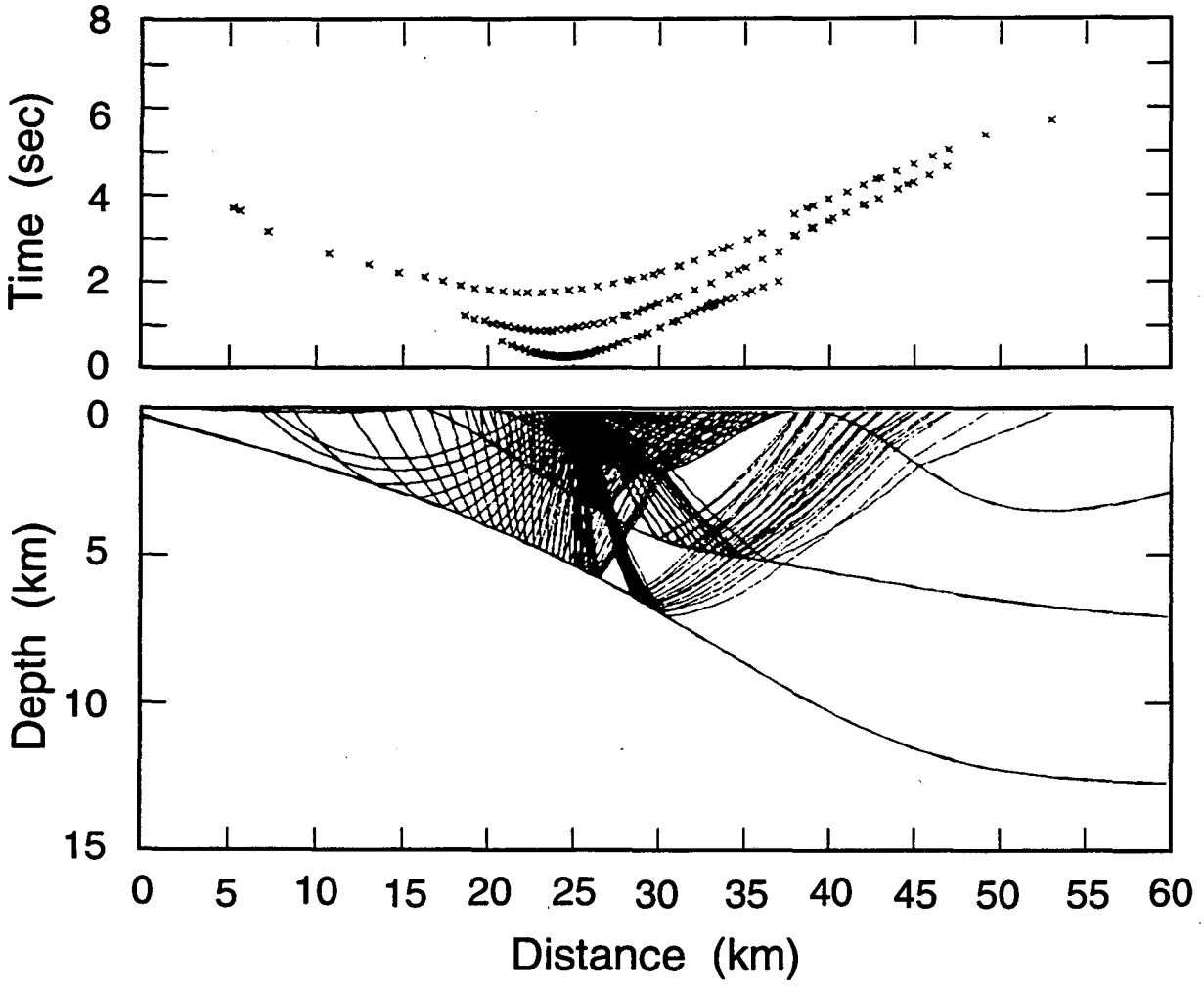

Fig. 4c Seismic rays and travel times including SWCC/Crescent interface using subduction model without anticline for SWCC. Velocities are given in text.

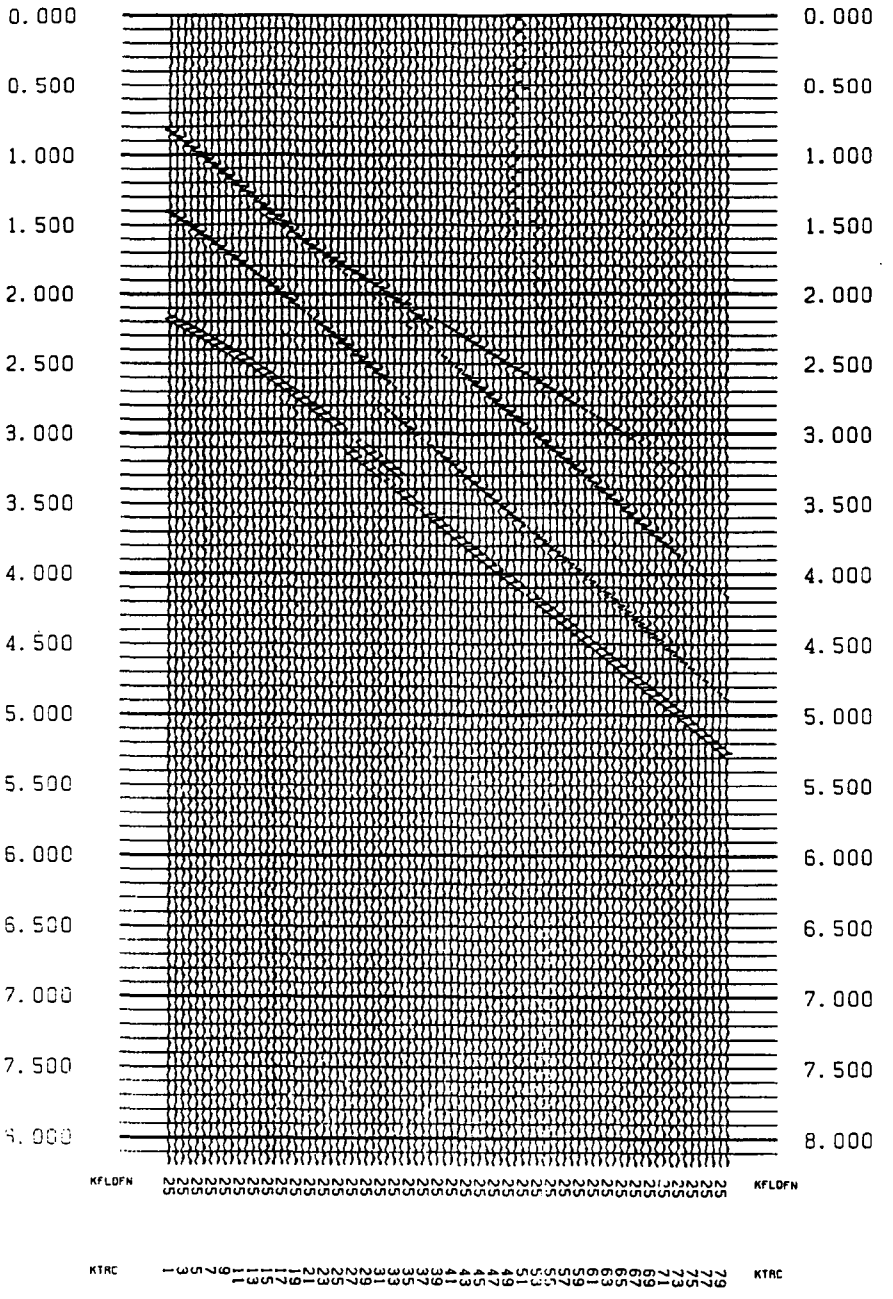

Fig. 4d Synthetic seismograms for source rays in Fig. 4c, AGC applied. Traces are spaced every 250 m east of the source.

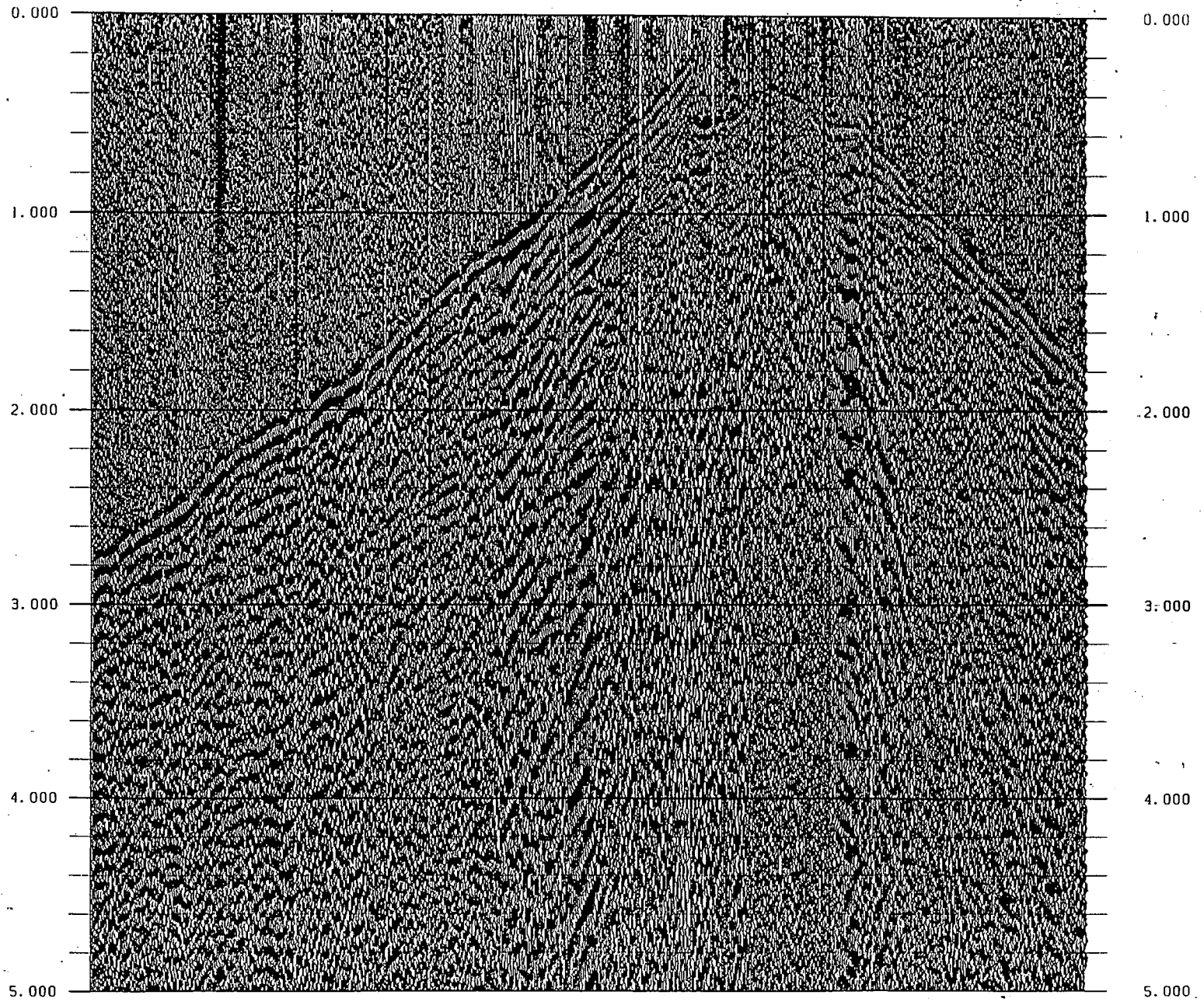

Fig. 5a Shot gather for a stack of four explosive shots about 1/2 mile off the east end of reflection line 5.

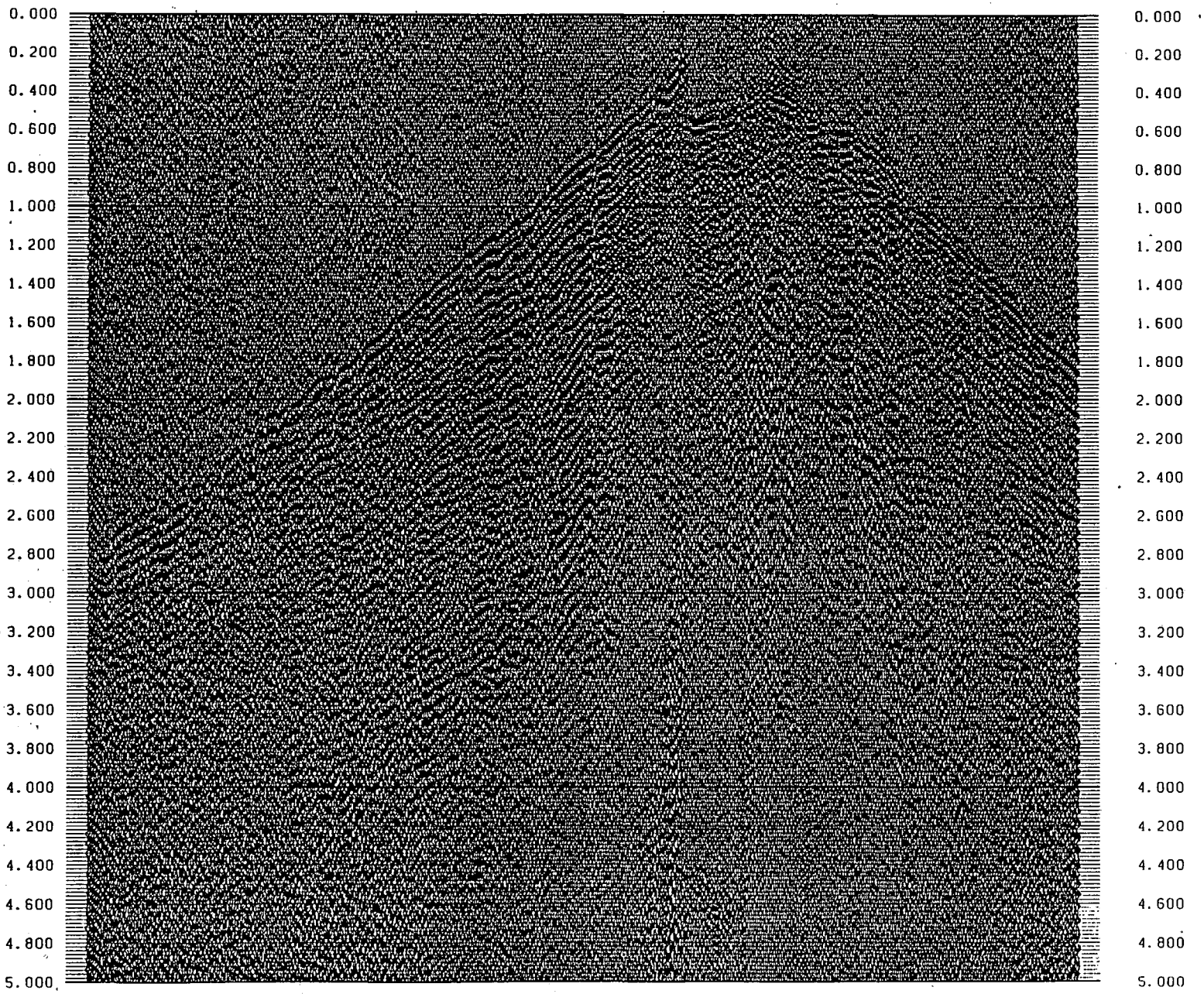

Fig. 5b Vibroseis shot gather with stack of 48 sweeps from the same source location as the explosive source Fig. 5a.

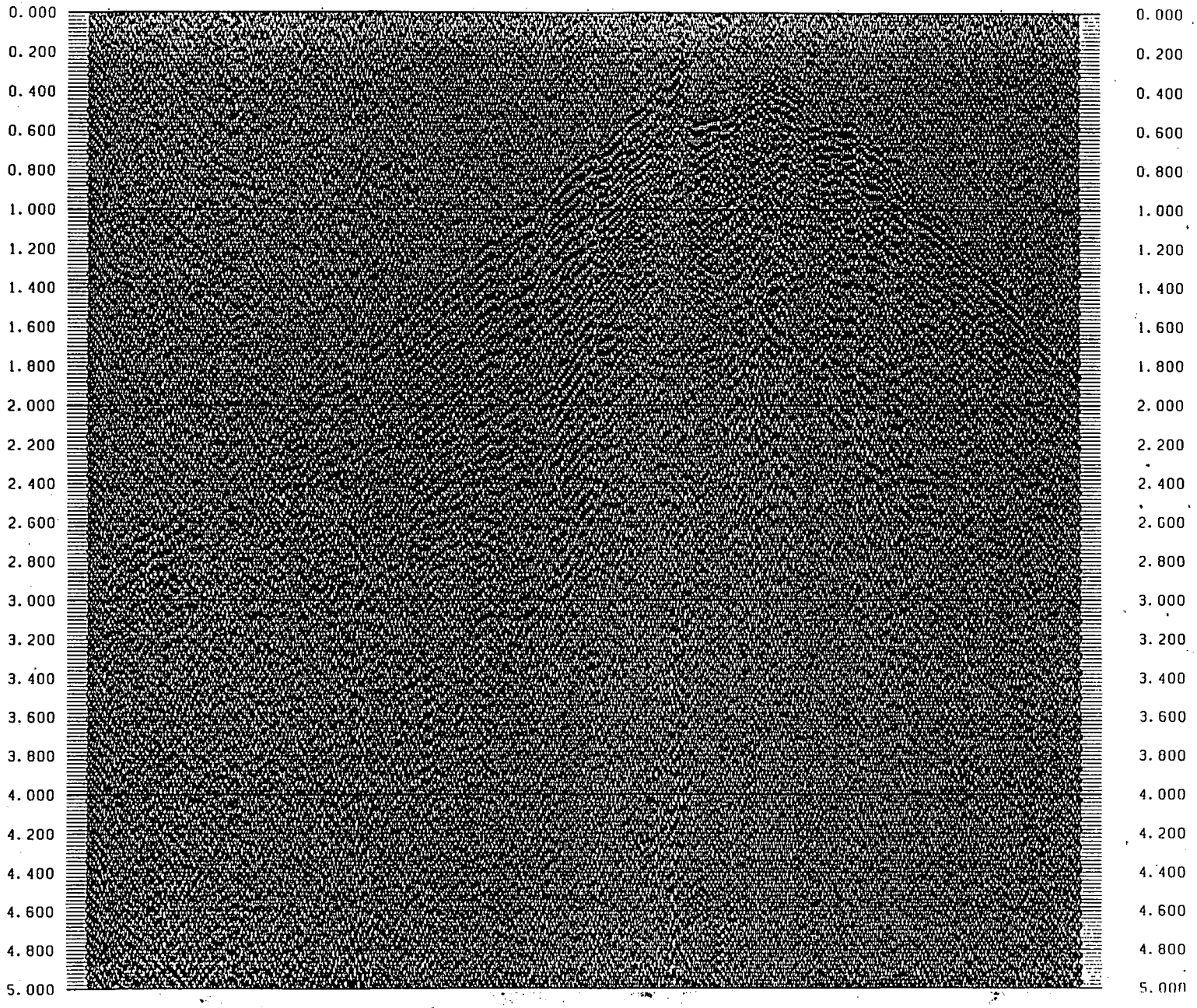

Fig. 5c Vibroseis shot gather with stack of 12 sweeps from the same source location as the explosive source Fig. 5a.

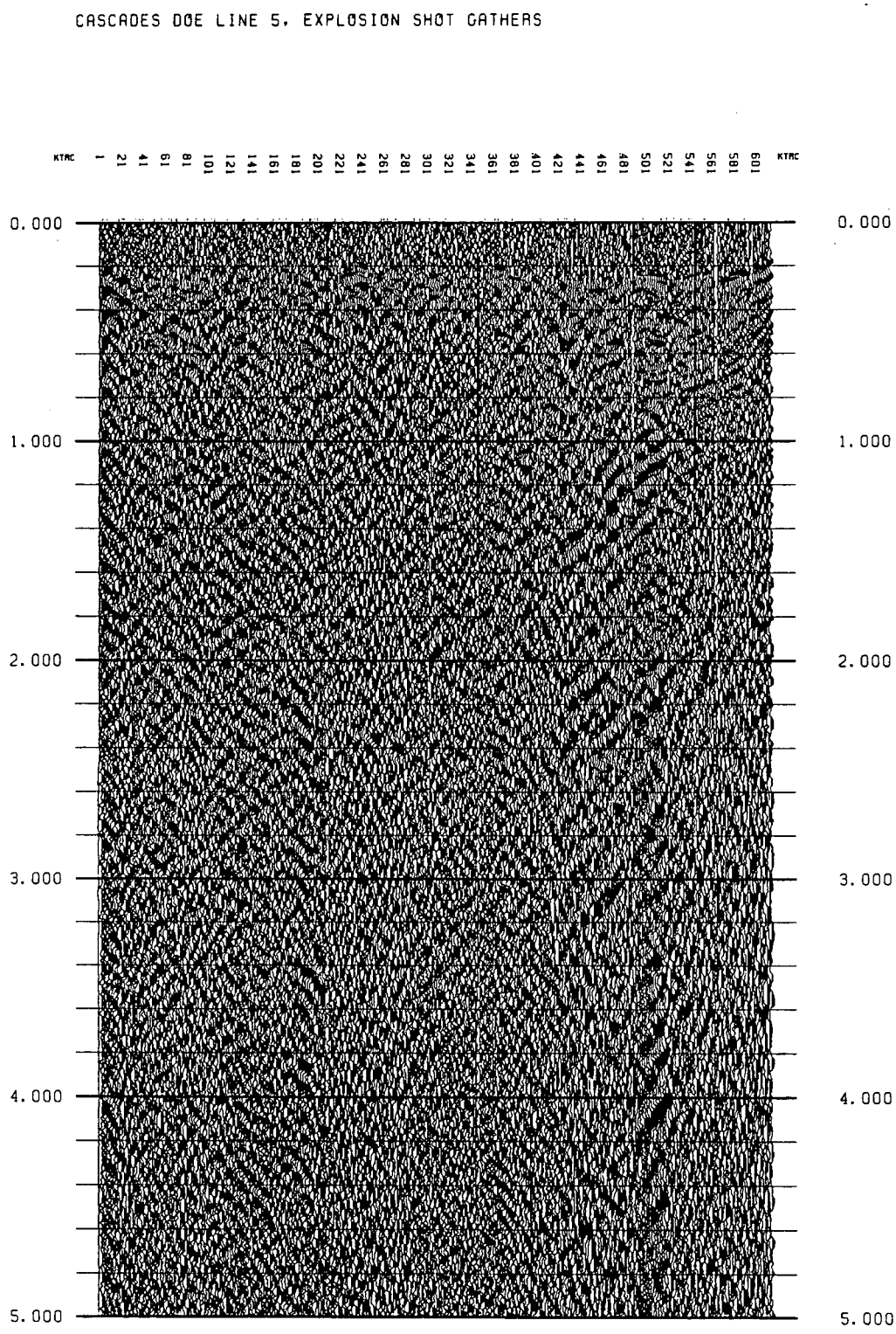

Fig. 6 West/East part of explosive shot gather (Fig. 5a), first arrival aligned at 0.2 s with elevation statics and refraction statics (refraction velocities were 3550 m/s and 4500 m/s), FK filtered to remove direct P-wave arrival and multiples.

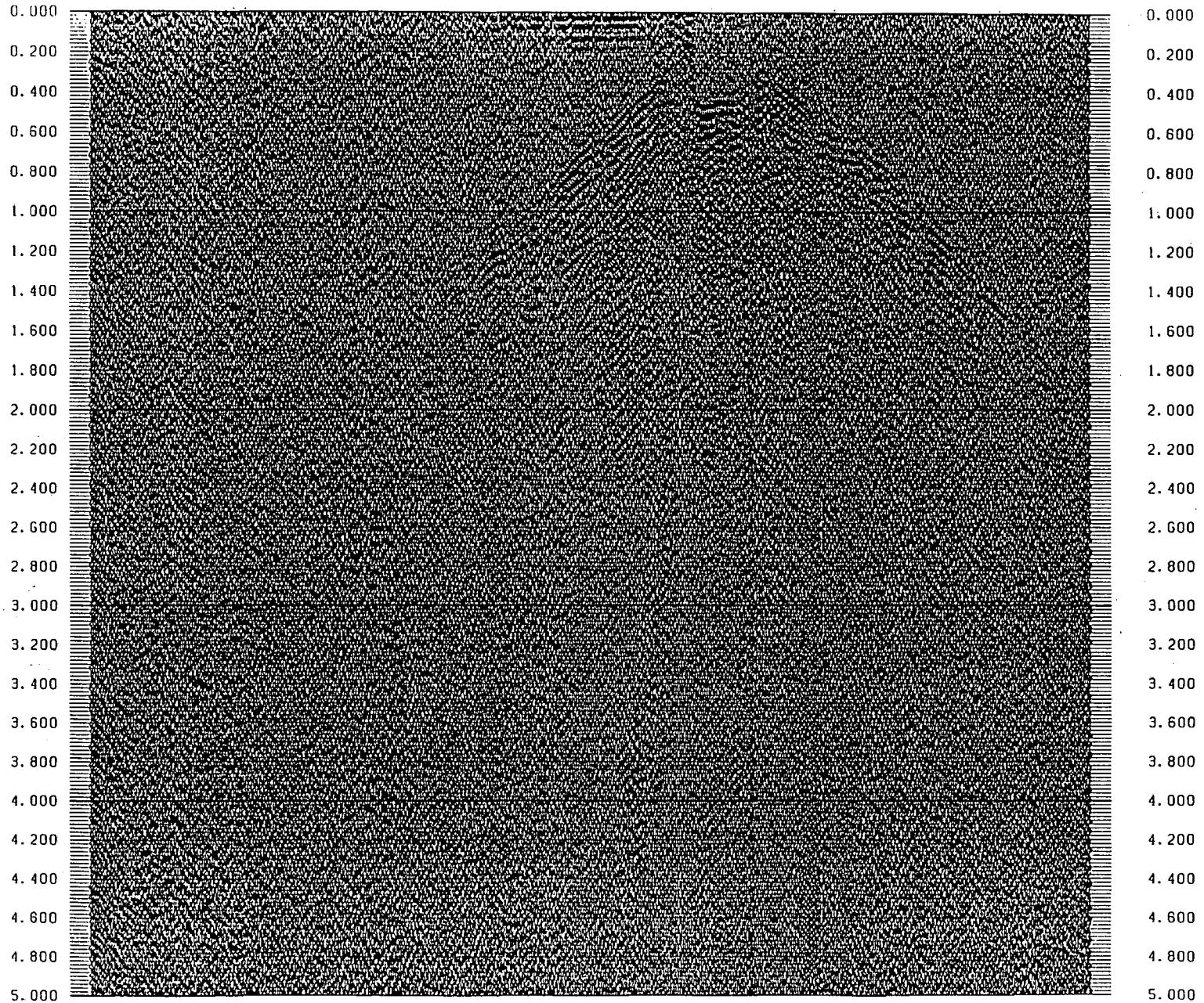

Fig. 7 Typical vibroseis shot gather from line 5 with a stack of 12 sweeps, shot point near to test shots in Fig. 5a, b and c.

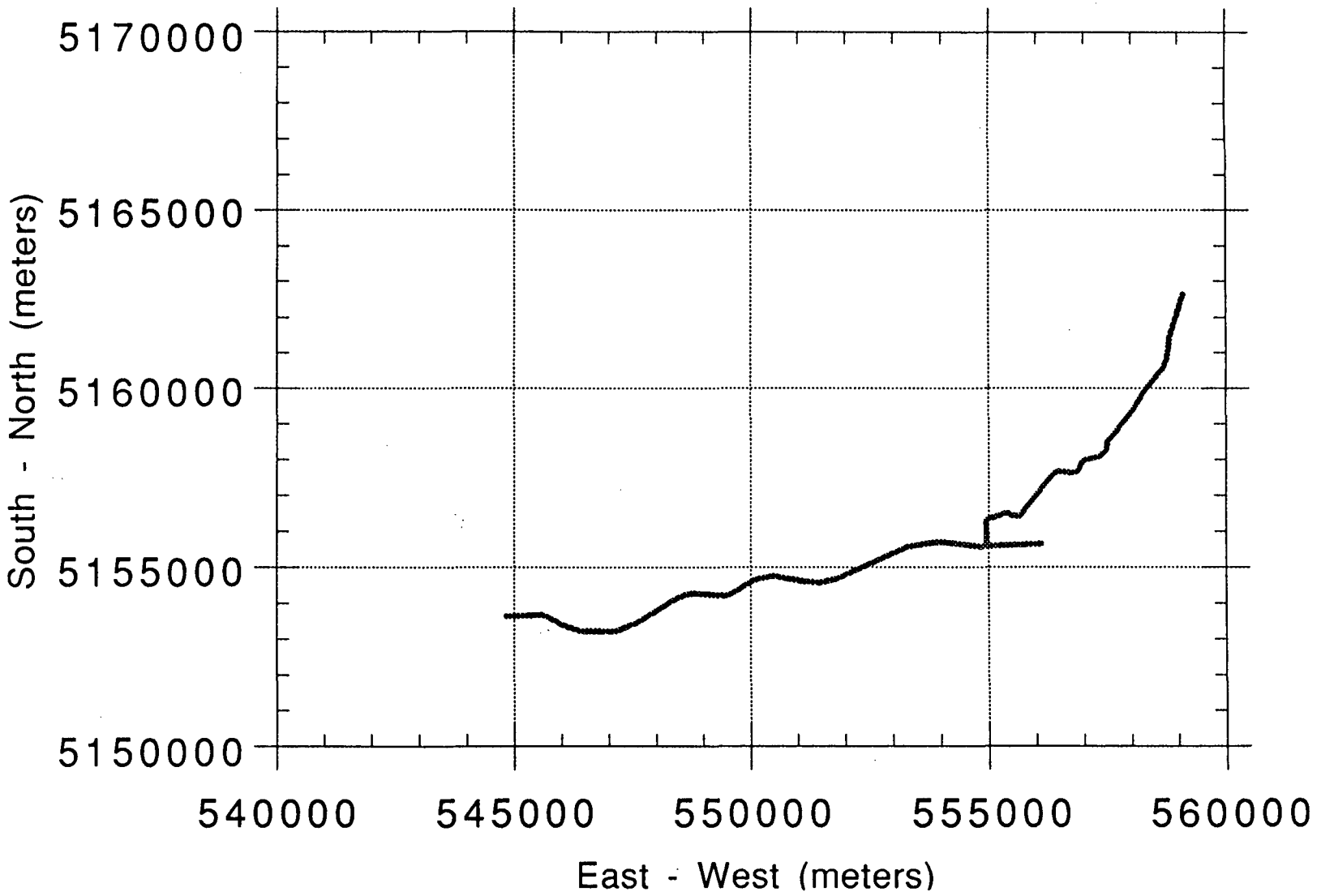

Fig. 8a Geometry of receivers and shot points for line 5.

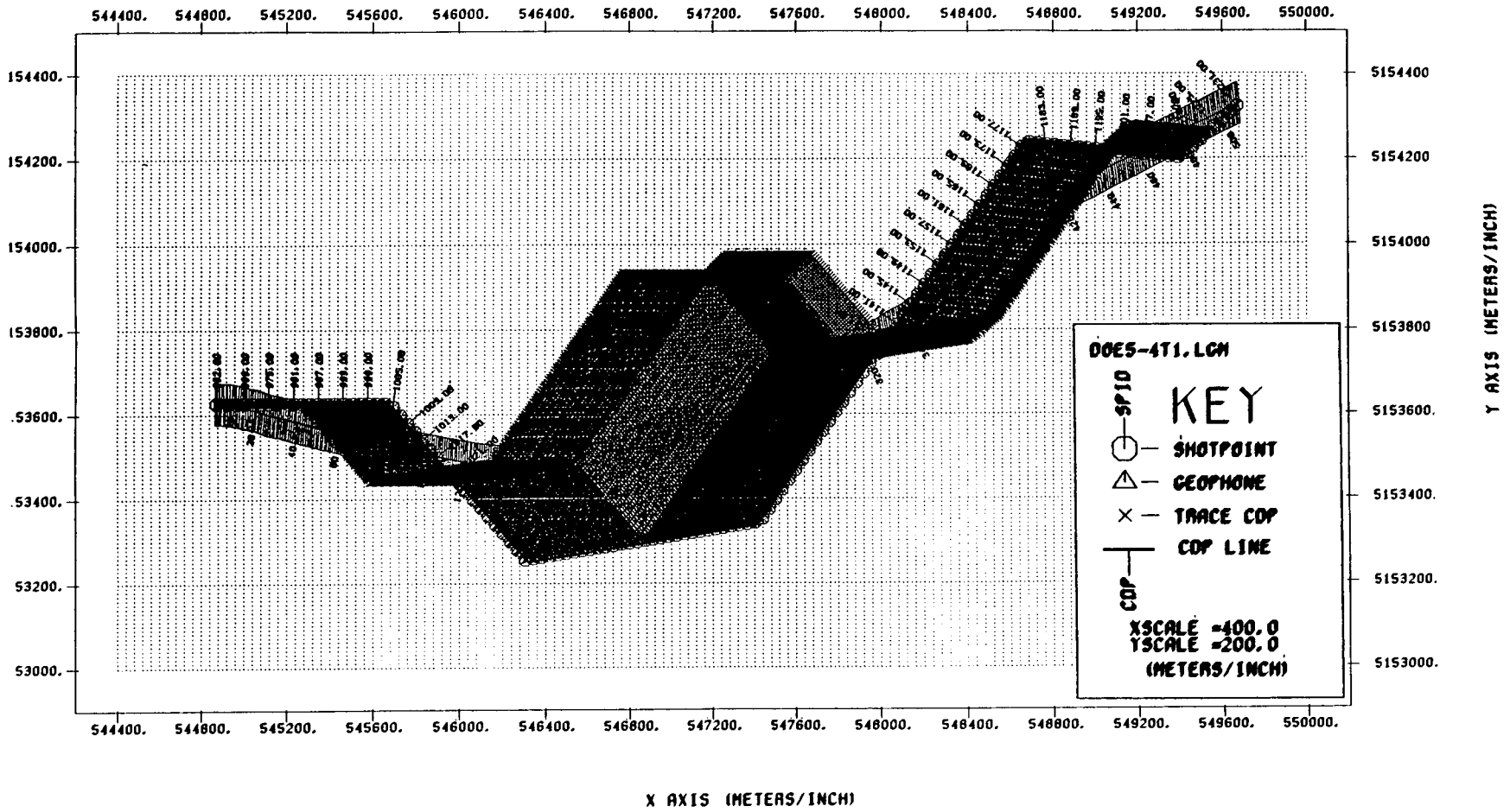

Fig. 8b West end midpoint locations used for brute stack of line 5.

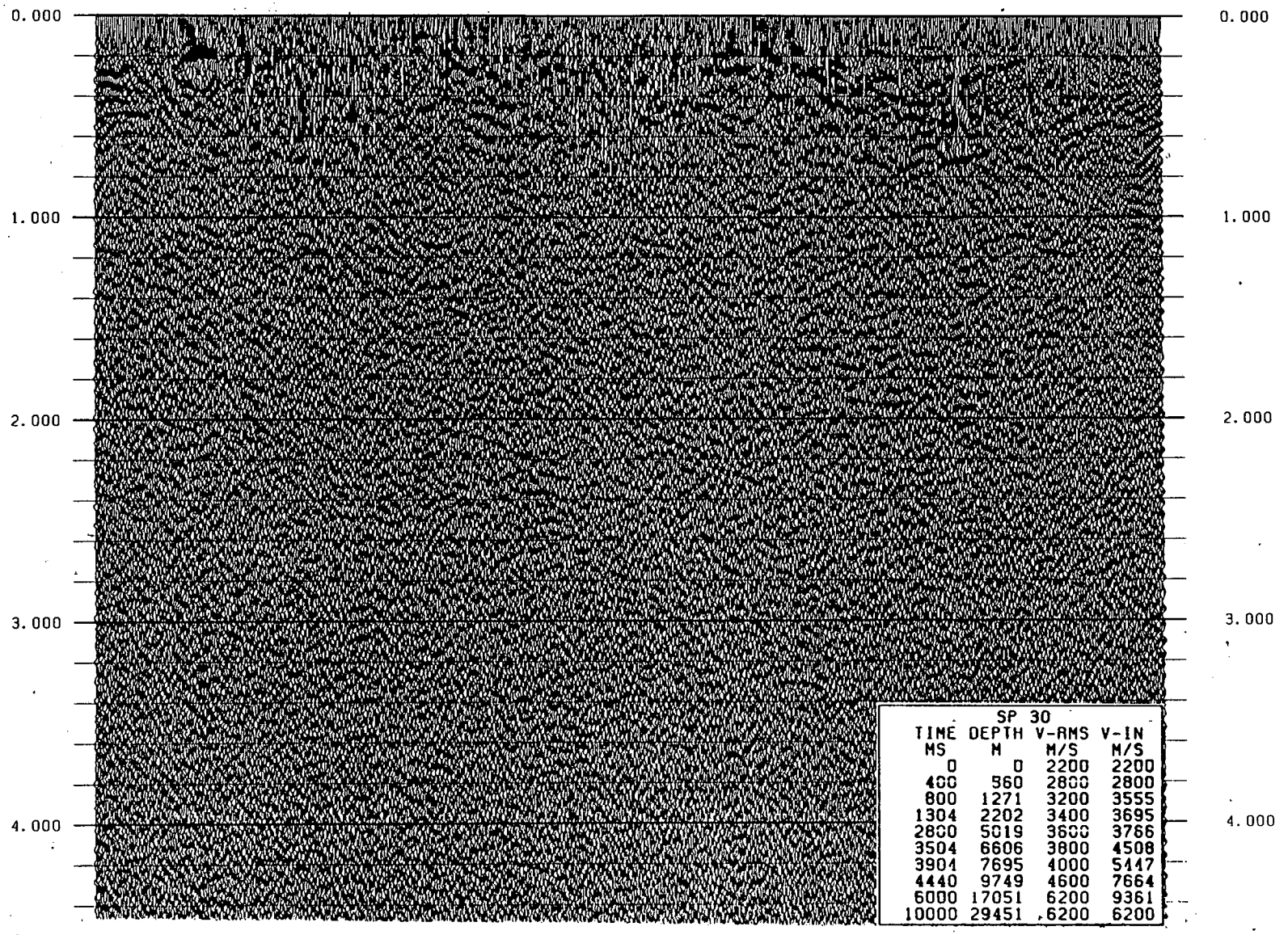

Fig. 9 Brute CDP stack of line 5 with 1 s AGC applied.

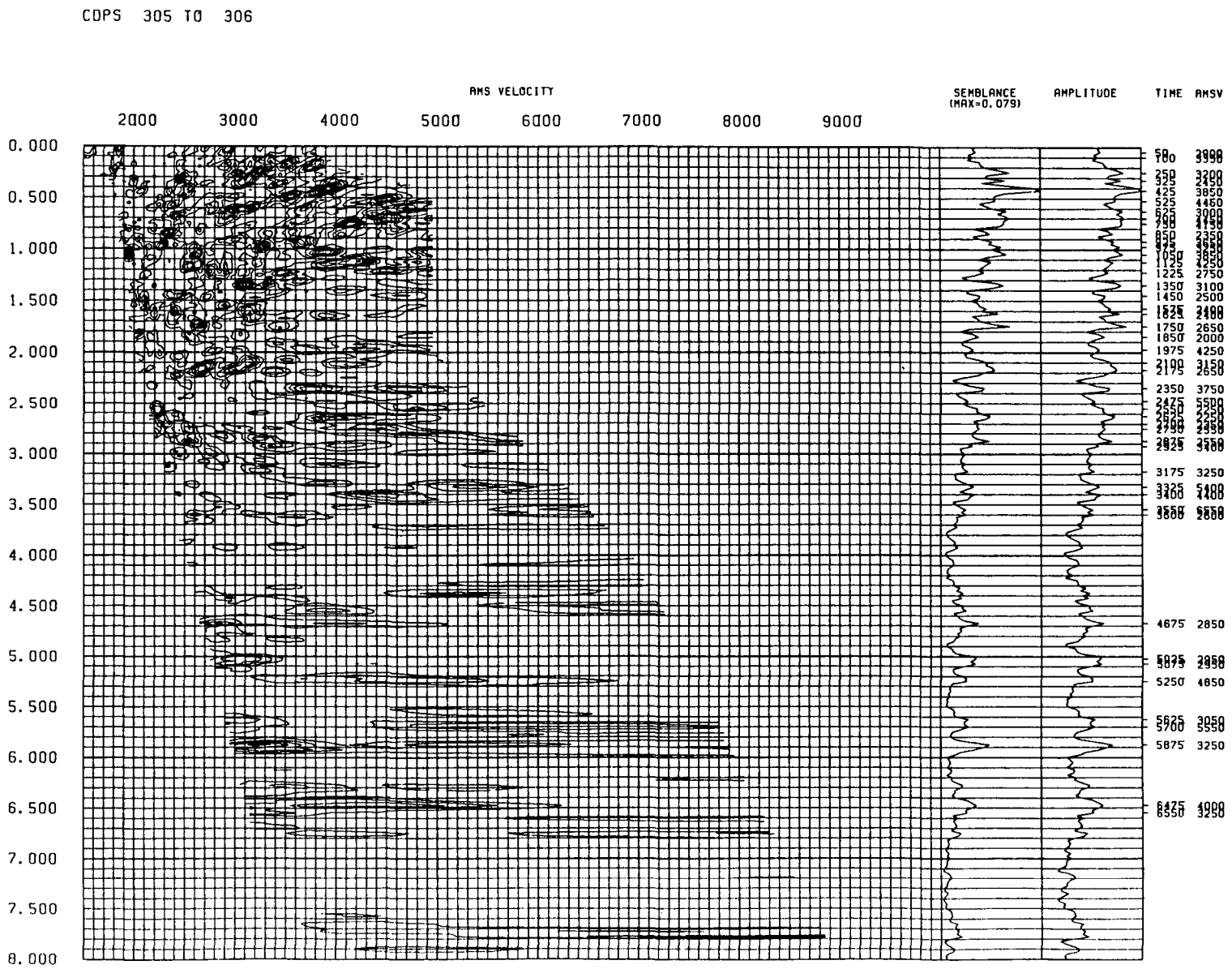

Fig. 10 Velocity semblance plot for two cdps from line 5, note the lack of coherent energy after about 4 seconds.

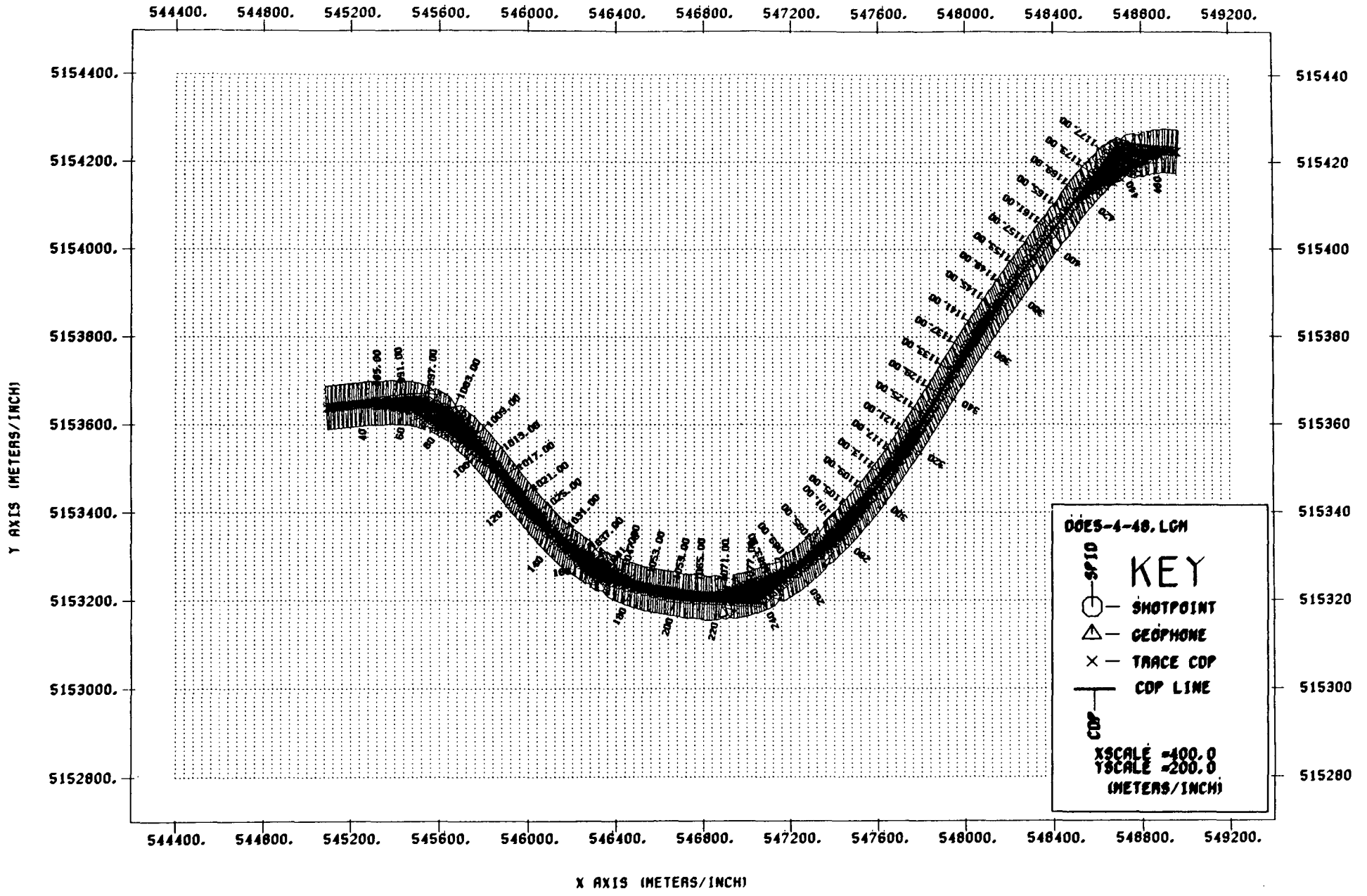

Fig. 11 Midpoint locations for 48 channel brute stack (Fig. 12). Compare with Fig. 8b. to see the reduced lateral smearing.

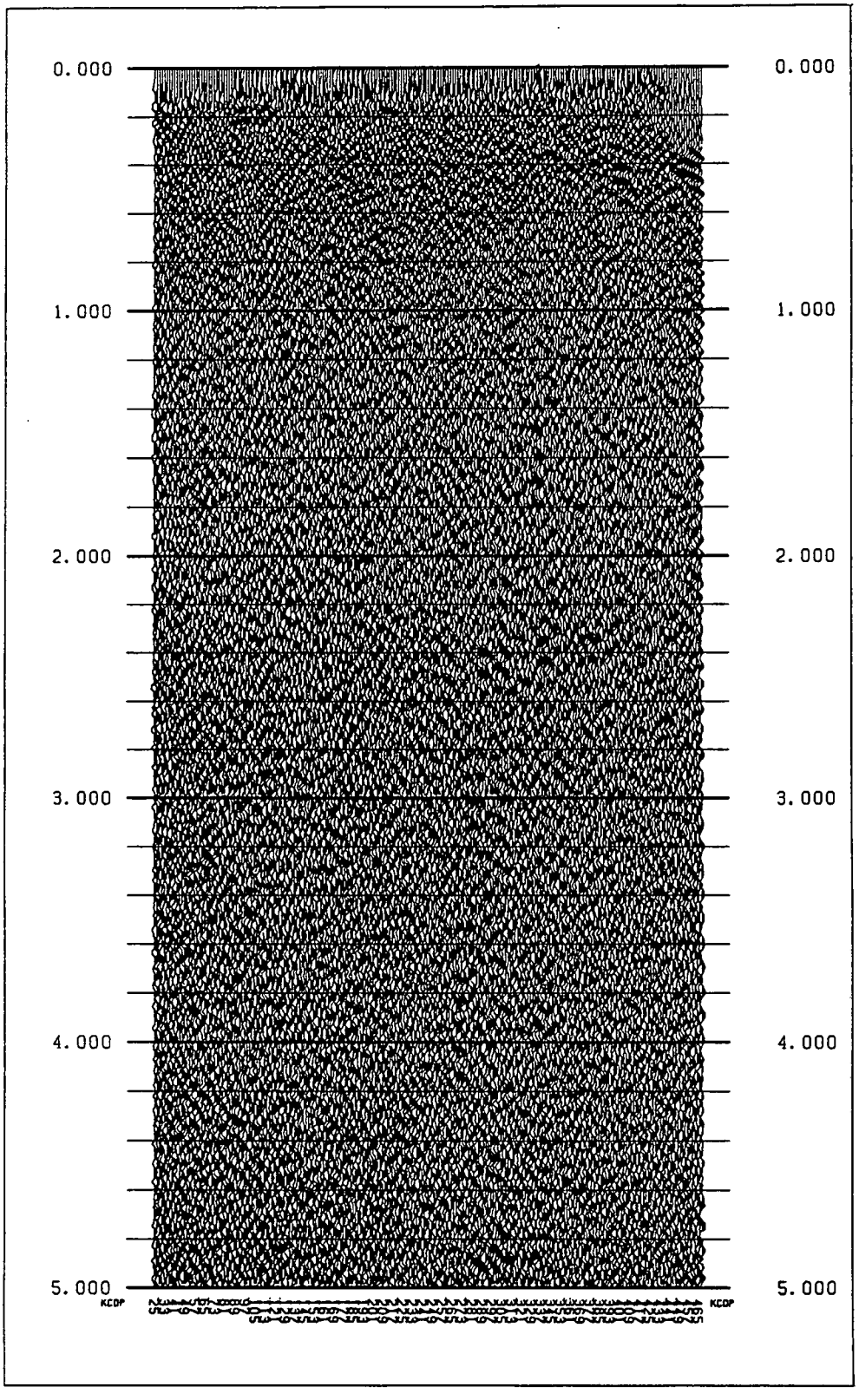

Fig. 12 Brute CDP stack of west end of line 5 using 48 channel shot gathers with 1 s AGC applied.

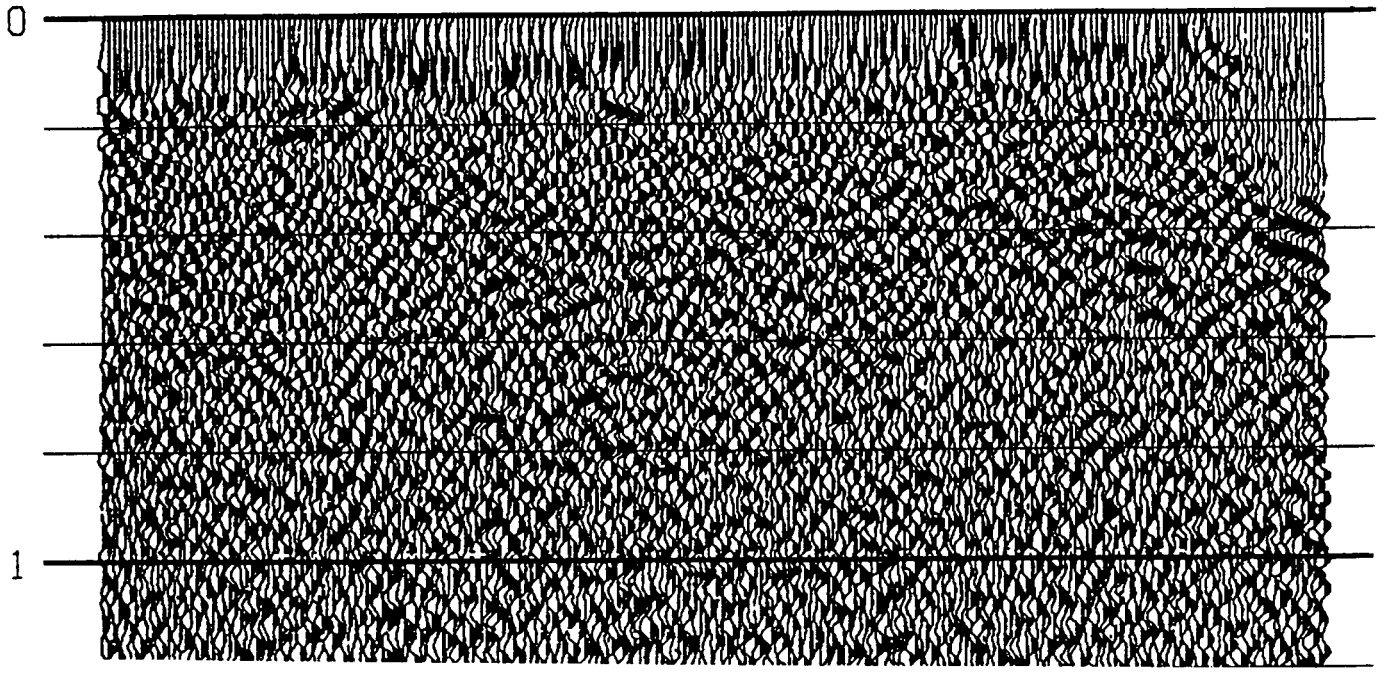

Fig. 13a Detail of first second of data from Fig. 9.

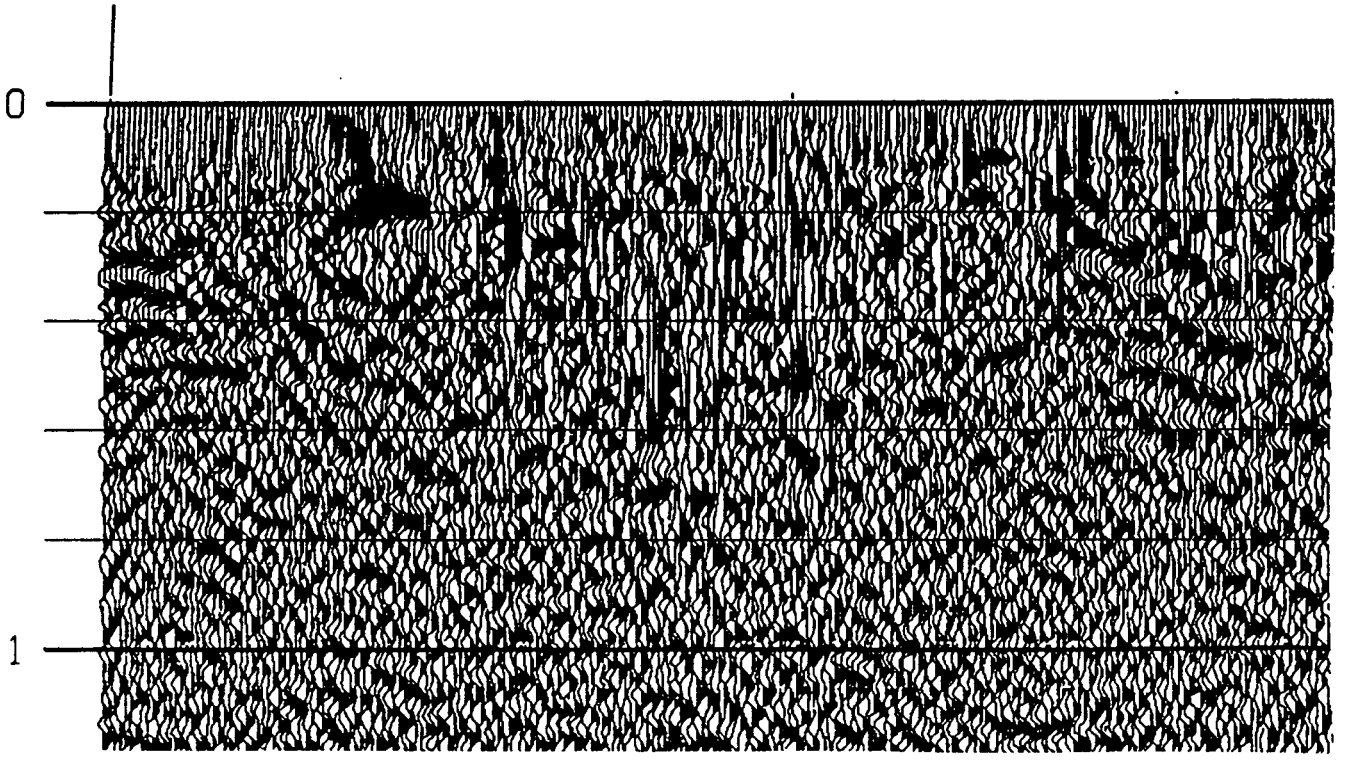

Fig. 13b Detail of first second of data from Fig. 12.

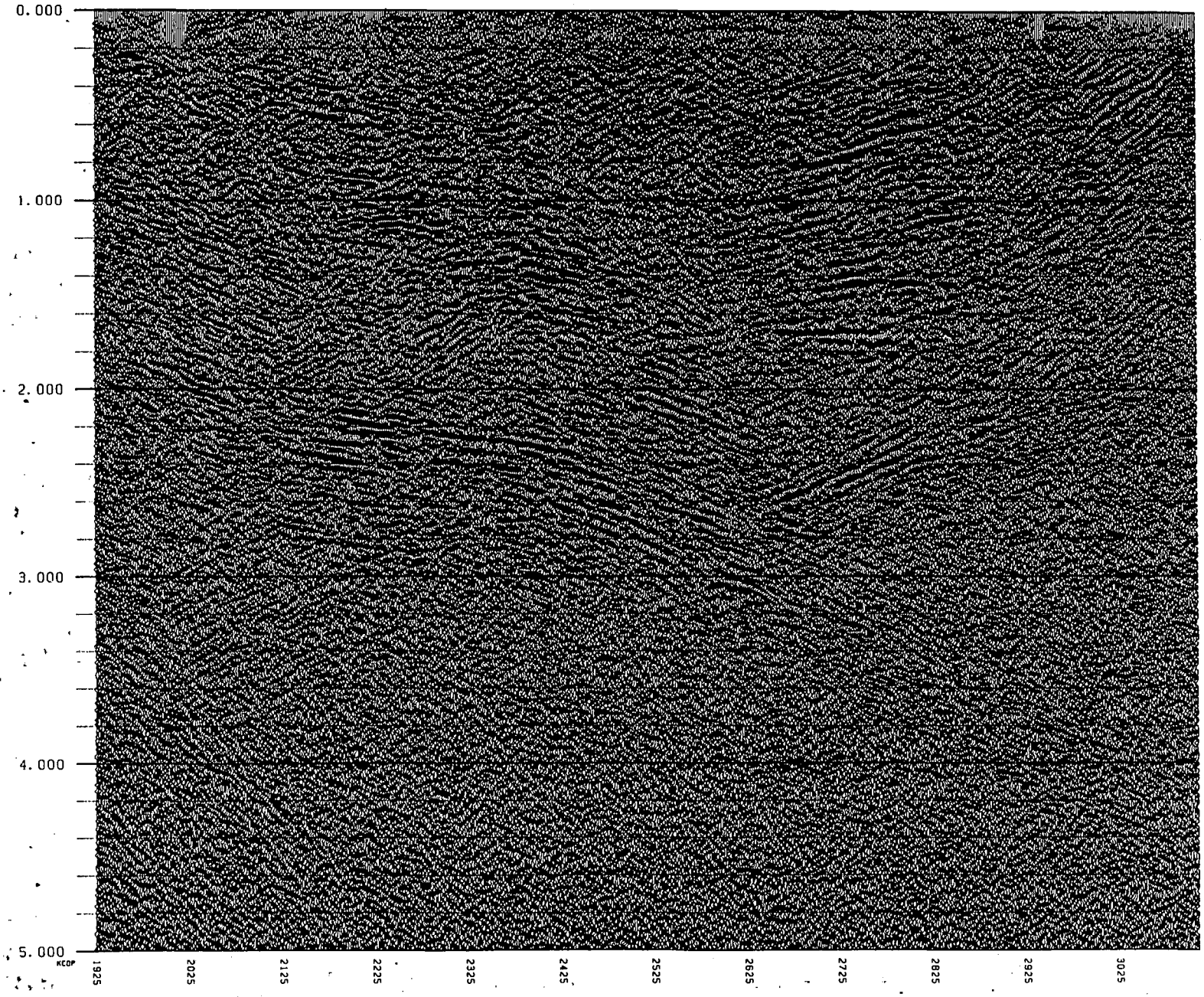

Fig. 14 Processed CDP stack of line 5 from Geotrace Technology.

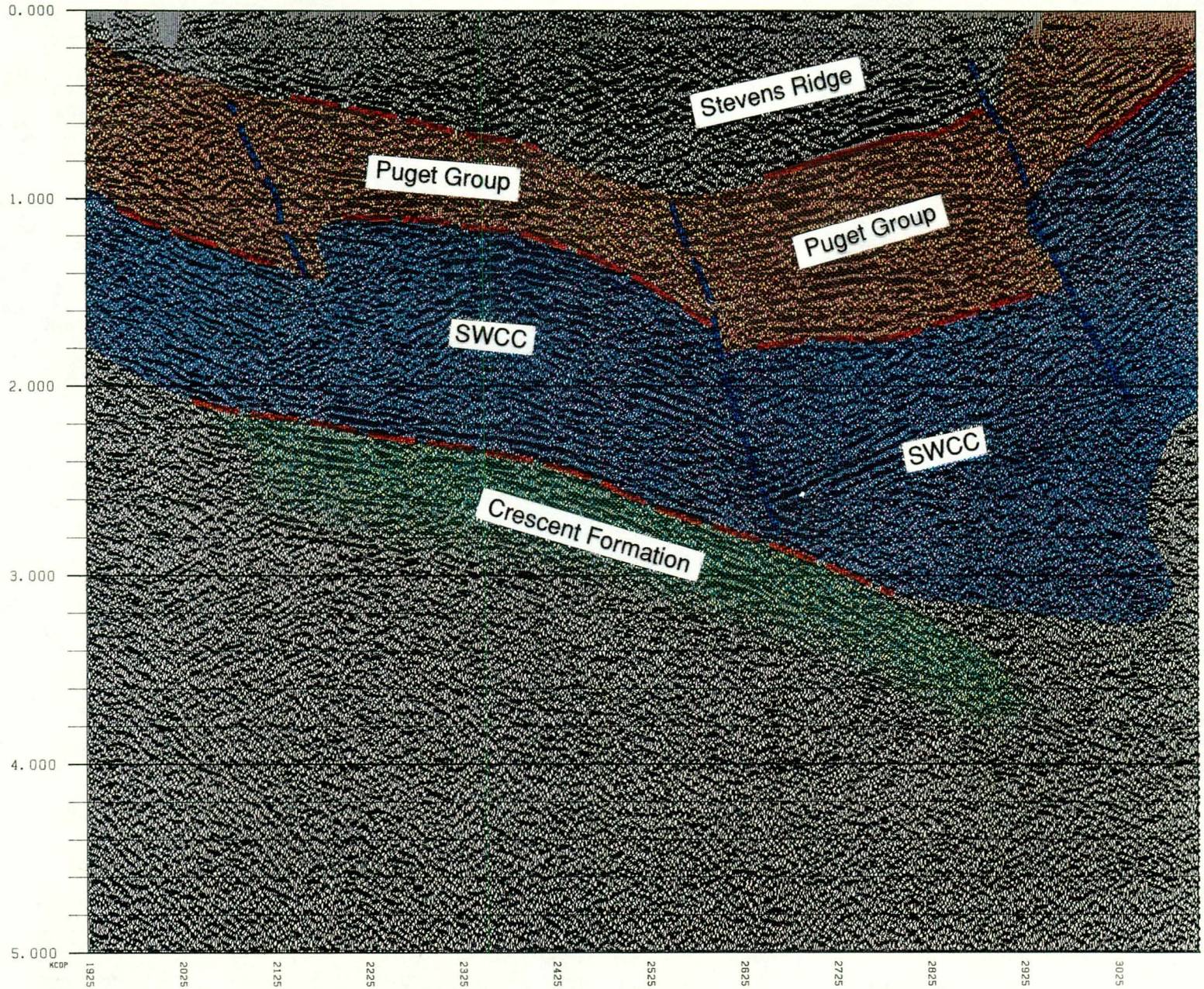

Fig. 15a Interpretation of Geotrace stack based on work of Stanley et. al. (1991) with SWCC continuous across section.

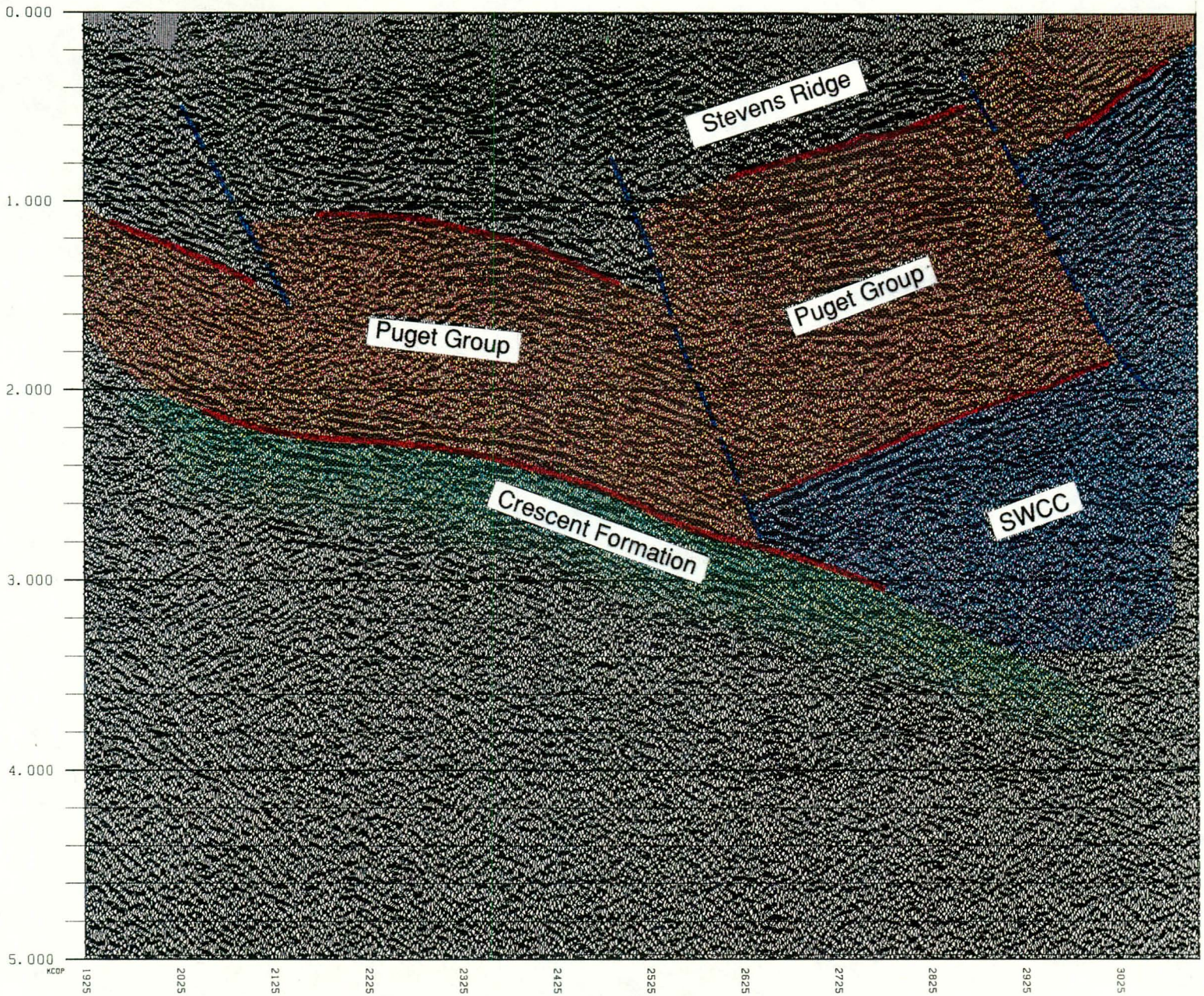

Fig.15b Interpretation of Geotrace stack based on a subduction model. Note the wedged pinch-out of SWCC which may correlate with the edge of the MT anomaly.

LAWRENCE BERKELEY LABORATORY
UNIVERSITY OF CALIFORNIA
TECHNICAL INFORMATION DEPARTMENT
BERKELEY, CALIFORNIA 94720